Single-molecule detection of transient dimerization of opioid receptors 2: Heterodimer blockage reduces morphine tolerance

Peng Zhou[1], Rinshi S. Kasai[2,3,4], Wakako Fujita[5,6], Taka A. Tsunoyama[1], Hiroshi Ueda[7,8], Simone Pigolotti[9], Takahiro K. Fujiwara[10], and Akihiro Kusumi[1,10]

[1]Membrane Cooperativity Unit, Okinawa Institute of Science and Technology Graduate University, Onna-son, Okinawa 904-0495, Japan. [2]Institute for Life and Medical Sciences, Kyoto University, Kyoto 606-8507, Japan. [3]Division of Advanced Bioimaging, National Cancer Center Research Institute, Tokyo 104-0045, Japan. [4]Institute for Glyco-core Research (iGCORE), Gifu University, Gifu 501-1193, Japan. [5]Department of Medical Pharmacology, Nagasaki University Graduate School of Biomedical Sciences, Nagasaki 852-8520, Japan. [6]Laboratory of Pharmacotherapeutics, Faculty of Pharmacy, Juntendo University. Urayasu, 279-0013, Japan. [7]Laboratory for the Study of Pain, Research Institute for Production Development, Kyoto 606-0805, Japan. [8]Department of Pharmacology, National Defense Medical Center, Nei-Hu 114, Taipei, Taiwan. [9]Biological Complexity Unit, Okinawa Institute of Science and Technology Graduate University, Onna-son, Okinawa 904-0495, Japan. [10]Institute for Integrated Cell-Material Sciences (WPI-iCeMS), Kyoto University, Kyoto 606-8501, Japan.

Graphical Abstract

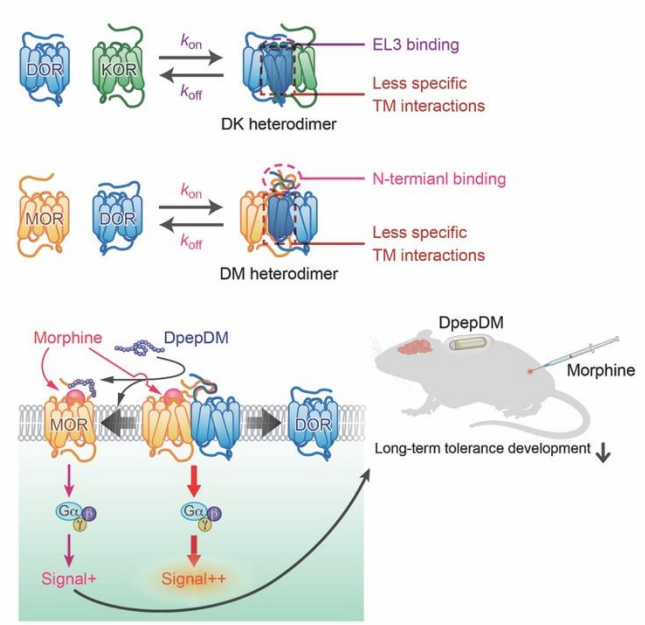

Highlights

- Transient δ-μ and δ-κ, not μ-κ, heterodimers of opioid receptors repeatedly form
- Heterodimerization sites exist in exodomains, and TM sites work less specifically
- Transient heterodimers of agonist-bound μ with δ emit stronger pulse-like signals
- δ-μ blocking peptide reduces tolerance after repeated morphine treatments in mice

Summary

Heterodimerization of opioid receptors (ORs), MOR, KOR, and DOR, is implied in their functional regulation and diversification, and thus its understanding is crucial for developing better analgesic treatments. However, our knowledge on OR heterodimerization/heterodimers remains limited. Here, using single-molecule imaging and functional analysis, we found that MOR, the main morphine receptor, repeatedly forms *transient (≈250 ms) heterodimers* with DOR every 1-10 seconds, but not with KOR, whereas DOR and KOR also form transient heterodimers. We obtained all the heterodimer-monomer equilibrium constants and rate constants with/without agonists. We identified the critical heterodimer binding sites in the extracellular domains, in addition to the less-specific transmembrane domains, and developed soluble peptide blockers for MOR-DOR and DOR-KOR heterodimerization, using amino-acid sequences mimicking the extracellular binding sites. With these peptide blockers, we dissected the monomer/dimer roles in OR internalization and signaling. The soluble MOR-DOR heterodimer blocker reduced the development of long-term morphine tolerance in mice.

Introduction

As elucidated in our companion paper,[1] the transient homodimerization of μ-, κ-, and δ-opioid receptors (KOR, MOR, and DOR, respectively) provides a critical layer of regulation within the opioid signaling paradigm. New theories and methods for quantitative analyses of single-molecule imaging data developed there revealed that all ORs undergo transient homodimerizations for brief periods of 120-180 ms (k_{off} = 6.7-8.5 s^{-1}), and they repeat dissociation and rebinding to another molecule every few seconds or less under physiological expression levels, with homodimer-dissociation equilibrium constants of 5.9-16.4 copies/μm^2. The homodimerization is predominantly driven by unique 9-26 amino-acid stretches within the C-terminal cytoplasmic domain of each receptor, with less specific contributions from the transmembrane (TM) domains. Soluble but membrane-permeable peptides mimicking these C-terminal regions reduced homodimerization, enabling us to dissect the functions of homodimers. Compared to their monomeric counterparts, KOR-KOR and DOR-DOR homodimers (KK and DD homodimers)—unlike MOR-MOR homodimers (MM homodimers)—activate downstream signals differently in response to agonist binding, without affecting receptor internalization.

In this paper, we extend these advanced single-molecule imaging studies described in the companion paper to investigate OR *hetero*dimerization. The heterodimerization of three classical ORs introduces a new dimension to receptor interactions with G proteins, GRKs, and arrestins,[2-6] providing additional opportunities for modulating OR functions. This modulation could be clinically utilized for managing chronic pain and treating neuropsychiatric disorders.[7-10]

Given its crucial role in morphine response and the significant medical and social implications thereof, MOR has been the focus of extensive OR research,[10-15] including its heterodimerization with DOR and KOR (DM and KM heterodimers, respectively).[10,13,16,17] Extensive studies have reported DM heterodimerization[3,18-20] and downstream signals suggesting DM interactions,[21-24] although DM co-expression might be limited to small populations of neurons, such as excitatory interneurons, projection neurons in the spinal cord

79 dorsal horn, and nociceptive neurons in dorsal root ganglia.[23,25,26] In contrast, evidence for KM
80 heterodimerization remains sparse, which suggests a dependence on the physiological
81 context.[17,27,28]

82 The DK coupling exhibited unique signaling and functional regulation, making the DK
83 heterodimer as another promising therapeutic target for pain treatment.[11,29,30] Indeed, DK
84 heterodimerization and observations suggesting DK interactions have also been
85 reported,[11,28,29,31,32] further highlighting its significance.

86 Despite these studies, the fundamental properties of heterodimers, including
87 heterodimer-monomer dissociation equilibrium constants and rate constants (K_D, k_{off}, which is
88 inverse lifetime, and k_{on}), heterodimer interaction sites, and cellular- and tissue-level functions,
89 remain enigmatic. This research addresses these fundamental issues by leveraging the
90 advanced single-molecule image analysis described in the companion paper. Such
91 understanding would form the basis for developing opioid analgesics with heightened efficacy
92 and minimized tolerance.

93 The heterodimer-monomer equilibrium constant, K_D (hetero-K_D), can only be obtained
94 after the homodimer-monomer equilibrium constants K_Ds (homo-K_Ds) for the two constituent
95 ORs are evaluated, as detailed in the companion paper. We also compare the properties and
96 dimerization sites between homo- and hetero-dimers of ORs.

97 This study lays the groundwork for future explorations of dimerization phenomena across
98 the broader GPCR family.[33,34] Heterodimerization among class-A GPCRs has been increasingly
99 observed, offering insights into novel signaling pathways and pharmacological profiles.[7,8,16,35,36]
100 Examples include heterodimers between MOR and V1b vasopressin receptor,[37] MOR and
101 somatostatin receptor 2,[38] dopamine D2 receptor and neurotensin NTS1 receptor,[39] angiotensin
102 II AT1 receptor and norepinephrine α2C-adrenergic receptor,[35] cannabinoid receptors CB1 and
103 CB2,[40] dopamine receptors D1 and D2,[41] and others, marking an emergent frontier in GPCR
104 research with profound implications for drug discovery.

105 Here, we unequivocally demonstrate that, under low physiological expression conditions,
106 DOR-MOR and DOR-KOR form metastable heterodimers, whereas MOR-KOR heterodimers are
107 not detectable. These findings have been substantiated through examinations conducted with
108 a level of quantification unparalleled in the existing biomedical literature, with the exception of
109 the OR homodimer research described in our companion paper.

110 Furthermore, we discovered that the extracellular N-terminal domain interactions and
111 extracellular loop 3 (EL3) interactions are specifically responsible for DM and DK
112 heterodimerizations, respectively. In contrast, the TM domain interactions contribute less
113 specifically, challenging the common belief that GPCR dimerizations are primarily mediated by
114 TM domain interactions.[3,16,30,42-44] In addition, allosteric conformational changes involving both
115 extracellular domains and TM domains might be involved.

116 Building on these findings, we demonstrated that soluble peptides mimicking the
117 extracellular amino-acid sequences implicated in DM and DK heterodimerizations effectively
118 inhibit heterodimer formation. In murine models, the administration of a soluble peptide blocker
119 targeting the DM heterodimers into the cerebral ventricles diminishes the development of long-
120 term morphine tolerance. These results strongly suggest that DM heterodimerization based on
121 the N-terminal domain sequence occurs in neuronal tissues. These findings underscore
122 potential avenues for improving opioid drug administration strategies aimed at mitigating
123 tolerance and dependence.
124

125 # Results

126 **Metastable DM and DK, but not MK, heterodimers are detected in the PM**

127 SNAPf-ORs and OR-Halos were expressed in CHO-K1 cells, which do not express ORs (Figures
128 S1A).[45] These tagged ORs are functional (Figures S1A and S1B) and labeled with SNAP-Surface
129 549 and Halo7-SaraFluor650T dyes. Their fluorescence characteristics are summarized in
130 Figures S1C-S1E. The labeled OR molecules were simultaneously observed in two colors at the
131 single molecule level at video rate (30 Hz) at 37°C, using a home-built total internal reflection
132 fluorescence (TIRF) microscope. The cells expressing each OR species at fluorescence spot
133 densities between 0.5-1 spot/μm^2 (total number densities between 1-2 spots/μm^2) after
134 fluorescence labeling were selected for microscope observations. Virtually all of the OR
135 fluorescent spots exhibited diffusion in the PM.

136 When DOR and MOR were expressed in the same cell, they exhibited frequent brief
137 colocalization and co-diffusion, suggesting metastable DM heterodimer formation (Movie S1
138 and S2; Figure 1A). For quantifying colocalization, we employed a pair cross-correlation function
139 (PCCF; Figure S1F; also see companion paper), which provides both a simple measure for
140 heterodimer formation, the colocalization index, and a fundamental constant, the heterodimer-
141 monomer dissociation equilibrium constant K_D (see Note S2, Figure S2E, and related main text
142 of the companion paper). As a control for incidental fluorescent spot colocalizations, the video
143 frames in the green channel were rotated 180° before overlaying (see Figure S2D of the
144 companion paper).

145 The colocalization index clearly indicated that DOR and MOR form DM heterodimers
146 (Figure 1B) and DOR and KOR form DK heterodimers (Figure 1B and S1F) in the PM (all
147 statistical parameters including p values and numbers of replicates are summarized in Table
148 S1, Excel format). However, at the expression levels employed in this study, KM heterodimers
149 were not detected (Figure 1B and S1F), consistent with the previous result.[28] The heterodimer-
150 monomer dissociation equilibrium constants K_D's were obtained from the PCCFs (Figure 1C).

151 The heterodimer lifetime (τ_2) was determined from k_{off} (summarized in Figure 1C),
152 evaluated from the distribution of colocalization *durations* (Figure 1D; see Note S1 in the
153 companion paper). The τ_2 values are 260 ± 12 ms for DM heterodimers and 241 ± 10 ms for
154 DK heterodimers, after corrections for trackable duration lifetimes (Figures 1D and S1E). The
155 histogram for the MK colocalization durations did not exhibit any τ_2 component (the decay
156 component representing the heterodimer loss), consistent with the lack of detectable
157 heterodimers for this pair (only incidental colocalization with a lifetime of τ_1; Figure 1D).
158 To identify the amino-acid sequences responsible for specific heterodimerization, we
159 initially examined the OR domains with lower amino-acid identities/homologies among the three
160 ORs. The candidate sites we initially selected are summarized in Figure 1E. The amino-acid
161 sequence homologies in the cytoplasmic C-terminal domains are lower, but they are not
162 included in this figure as they are involved in KK, MM, and DD homodimerizations (companion
163 paper) and we unequivocally showed that they are not involved in DK and DM
164 heterodimerizations (Figures 2A and 3A).
165

166 **DOR's EL3, TM1, and TM4, but not EL2, N- or C-terminal domain, contribute to DK**
167 **heterodimerization**

168 We first examined heterodimerization of wild-type (WT) KOR and N- or C-terminal deletion
169 mutants (ΔN or ΔC mutants) of DOR (Figure 2A, Top). We found that DOR's N- and C-terminal
170 domains are not involved in DK heterodimerization, and KOR's ΔN or ΔC mutations are not
171 involved in heterodimerization with WT-DOR (Figure 2A, Bottom). These results indicate that
172 DK heterodimerization involves neither the N- nor C-terminal domains of DOR and KOR.
173 Given the scarce occurrence of MK heterodimers (colocalization index = 1.15 ± 0.03), we
174 tested whether MOR mutants with some domains substituted with DOR counterparts could
175 heterodimerize with WT-KOR (Figure 1E; see Figure 2B for domain names and amino-acid
176 numbers; results shown in Figure 2C left). Substitution with DOR's TM1 or TM4 domain in MOR
177 (MOR[TM1^{DOR}] or MOR[TM4^{DOR}]) facilitated heterodimer formation with WT-KOR, qualitatively

178 consistent with a previous result.[30] However, replacing MOR's EL2 or N-terminal domain
179 (MOR[EL2^{DOR}] or MOR[Nterm^{DOR}]) did not induce heterodimerization with WT-KOR. Meanwhile,
180 introducing DOR's EL3 domain into MOR (MOR[EL3^{DOR}]) resulted in heterodimerization with
181 WT-KOR. These results indicate the involvement of DOR's EL3 domain, alongside its TM1 and
182 TM4 domains, in DK heterodimer formation.

183 The lifetime distribution for the MOR(EL3^{DOR})-KOR heterodimer revealed the appearance
184 of the τ_2 component, which did not exist in that for the MK pairs (Figure S2). Although the τ_2
185 value is smaller than that for WT-DK heterodimers (164 ± 25 ms vs. 241 ± 9.7 ms), this result
186 further suggests that DOR's EL3 domain is involved in DK heterodimerization.

187 Experiments replacing various DOR domains with the MOR counterparts and examining
188 heterodimerization with WT-KOR (based on the lack of MK heterodimerization) showed reduced
189 heterodimerization for TM1, TM4, and EL3 domain replacements, but not for EL2 or N-terminal
190 domain substitutions (Figure 2C right). This further indicates that DOR's EL3, TM1, and TM4
191 domains are integral to DK heterodimer formation.

192

193 **Soluble EL3-domain peptides of DOR and KOR both block DK dimerization**

194 A variety of deletions (Figure 2A) and substitutions (Figure 2C) introduced into WT-DOR could
195 alter its conformation, which might affect true interaction sites, leading to the reduction of DK
196 heterodimerization. To study this aspect, we synthesized soluble peptides with the EL3
197 sequences of DOR and KOR (Figure 1E). Addition of either peptide (1 μM, final concentration)
198 to cells co-expressing DOR and KOR significantly reduced DK heterodimerization, unlike the
199 peptide with the MOR EL3 sequence (Figure 2D). This highlights the critical roles of the DOR
200 and KOR EL3 domains in DK heterodimerization. Given that DOR's EL2 domain and the N-
201 terminal domains of both DOR and KOR are not involved in DK heterodimerization (Figures 2A
202 and 2C), these results indicate that the interaction between the DOR and KOR EL3 domains is
203 crucial for DK heterodimerization, although that with KOR's EL2 domain has not been ruled out.

204 Furthermore, we found that DOR's TM1 and TM4 peptides expressed in the PM became
205 colocalized with KOR, supporting their involvement in DK heterodimerization (Figures 2B and
206 2E). These results are consistent with those shown in Figure 2C and a previous observation,[31]
207 and indicate that the interactions between the DOR and KOR EL3s, and those of DOR's TM1
208 and TM4 with KOR's TM domains are involved in DK heterodimerization.
209

210 **DM dimerization is predominantly mediated by N-terminal domain interactions**

211 To identify the amino-acid sequences responsible for DM heterodimerization, first, we
212 systematically deleted partial sequences from the N- and C-terminal domains of DOR and MOR
213 (Figure 3A). We found that DOR's N-terminal amino acids 22-42 (with the critical amino acids
214 22-27) and MOR's N-terminal amino acids 32-61 play key roles in DM heterodimerization, likely
215 by binding to each other (Figure 3A). The key DOR sequence was further confirmed by replacing
216 DOR's amino acids 21-27 with an arbitrarily selected amino-acid sequence, rather than deleting
217 the original sequence (Figure S3). Therefore, these sequences are likely to be the binding
218 interfaces for DM heterodimerization. However, the colocalization index did not decrease to 1
219 (but to 1.15, as found for MK heterodimerization), probably due to the presence of other
220 binding sites such as TM domains, as suggested previously (see below).[3,43,46]

221 The histograms of the colocalization *durations* for DORΔ22-42 with WT-MOR and
222 MORΔ32-61 with WT-DOR both revealed only small fractions of the τ_2 components, with
223 significantly reduced heterodimer lifetimes of 88 ± 12 ms and 91 ± 8 ms, respectively (Figure
224 3B). These shorter lifetimes (≈90 ms), compared to the 260-ms lifetime of the WT DM
225 heterodimers, might represent the lifetimes of DM heterodimers induced by the less-stable TM
226 domain interactions.

227 We further explored the specific regions mediating DM heterodimerization by taking
228 advantage of the fact that MK heterodimerization hardly occurs at the expression levels we
229 employed. Thus, we examined WT-MOR interactions with DOR mutants with various DOR
230 domains substituted with their KOR counterparts (Figure 3C left). The colocalization index upon

231 replacement of the N-terminal domain substantially decreased, consistent with the previous
232 demonstration that the N-terminal domains of DOR and MOR are instrumental in DM
233 heterodimer formation (Figures 3A and 3B).

234 Substitution of DOR's TM1 or TM4 with its KOR counterpart, but not TM6 (Figure 1E),
235 yielded moderate reductions in colocalization with WT-MOR, but not as much as the N-terminal
236 domain substitution (with $Nterm^{KOR}$), suggesting that DOR's TM1 and TM4 play ancillary roles
237 in DM heterodimer stability (Figure 3C left). These results, but not that of TM6, are consistent
238 with previous computational modeling predictions.[43,46] The DOR mutant bearing the three
239 replacements of KOR's N-terminal domain, TM1, and TM4 exhibited a lower colocalization index
240 with WT-MOR, comparable to that for the MK hetero-pair (1.15).

241 Conversely, the replacement of MOR's N-terminal domain with that from KOR (with
242 $Nterm^{KOR}$) greatly reduced the colocalization with DOR (Figure 3C right). This result further
243 supports the idea that the major interaction sites for DK dimerization do not involve the N-
244 terminal domains, but the key interactions occur between the EL3 domains as well as TM
245 domains in DOR and KOR (Figure 2). Importantly, it further demonstrates that the predominant
246 interactions for DM heterodimerization occur between the N-terminal domains of both DOR and
247 MOR (Figures 3A and 3B). The interactions of the N-terminal domains with the EL2 and EL3
248 domains would be far less important for DM heterodimerization than those between the DOR
249 and MOR N-terminal domains, because the lack of either DOR residues 22-42 or MOR residues
250 32-61 is sufficient to significantly lower the colocalization index (Figure 3A) and eliminate the
251 second colocalization lifetime component (Figure 3B).

252

253 **TM interactions enhance both homo- and hetero-dimerizations of ORs**

254 The results described in the previous subsection further support the involvement of DOR's TM1
255 and TM4 in both DM (Figure 3C left) and DK (Figures 2C, left and right, and 2E)
256 heterodimerizations. Furthermore, MOR's TM1 participates in both DM heterodimerization and
257 MM homodimerization (Figures 5B-5E in companion paper; Figure 5 of this paper). These

258 results suggest that the TM interactions support both homo- and hetero-dimerizations of ORs;
259 namely, the TM interactions are less specific. This finding is aligned with previous controversial
260 reports: The conclusion we obtain from the reported results in the literature is that the same
261 TM domains contribute to both homo- and hetero-dimerizations of ORs and other GPCRs to
262 various extents.[43,44,46-48]
263

264 **Soluble N-terminal-domain peptides block DM heterodimerization**

265 We then utilized the soluble peptides corresponding to the N-terminal sequences of both DOR
266 and MOR implicated in DM heterodimerization, as we did for confirming the DK heterodimer
267 binding sites (EL3 domains of both molecules; Figure 2D). These soluble peptides from DOR
268 and MOR are called Dpep(m-n)DM and Mpep(m-n)MD, respectively, where m and n indicate
269 the amino acid numbers in the original OR sequences (see "Location in DOR" and "Location in
270 MOR" in Figure 4A, respectively). Among the various DpepDMs and MpepMDs, Dpep(20-42)DM
271 and Mpep(32-61)MD most potently lowered the colocalization indexes to 1.2-1.3 (Figure 4A),
272 mirroring the effects observed with the deletion and replacement mutants (Figures 3A and 3C).

273 The colocalization index for DM heterodimers decreased with an increase in the Dpep(20-
274 42)DM concentration (Figure 4B), indicating that the affinity of the DM heterodimers is $K_D \approx 0.1$
275 μM in three-dimensional space. This 3D concentration could not readily be converted to a two-
276 dimensional molecular density, as discussed in the companion paper (main text explaining
277 Figures 5A-D). Briefly, in two-dimensional space, the dimerization efficiency is far greater, by
278 a factor of 10^6, than that in three-dimensional space.[49] Therefore, the efficacy of the peptides
279 in blocking OR dimerization, even at the 0.1 μM-order concentrations required for blocking DM
280 heterodimerization, is deemed plausible given the nanomolar affinity range of OR ligands (1-
281 10 nM).

282 Dpep(20-42)DM's introduction substantially shortened the DM heterodimer lifetime from
283 260 ms to 124 ms (Figure 4C), supporting that the amino acid sequence 20-42 in DOR is critical

284 for DM heterodimer formation. The shortened lifetime might reflect heterodimer facilitation by
285 the TM domains.
286
287 **The membrane-integral peptide TM1^{MOR} suppresses both DM heterodimerization**
288 **and MM homodimerization**
289 Next, we examined whether MOR's TM1 (TM1^{MOR}) is involved in DM heterodimerization, as
290 previously described.[3,43,46] In addition to TM1^{MOR} (amino acids 71-99), a second construct
291 containing amino acids 53-70 before the TM1 domain (Nterm- TM1^{MOR}) was used (see Figure
292 2B for construct names and exact amino-acid ranges), following a previous report.[3] When these
293 peptides were co-expressed with DOR, both TM1^{MOR} and Nterm-TM1^{MOR} colocalized with DOR,
294 like the full-length MOR (all molecules expressed at densities of 0.5-1.0 fluorescent spots/μm^2;
295 Figures 5A and 5B). These TM1 constructs also suppressed DM heterodimerization in an
296 expression level-dependent manner, indicating TM1^{MOR}'s significant contribution to the DM
297 interaction (Figure 5C).
298 Notably, the addition of either Dpep(20-42)DM (also Mpep(32-61)MD) or TM1^{MOR} alone
299 reduced the colocalization index to near-baseline levels (1.2-1.3) (Figures 4A, 4B and 5C).
300 These results suggest that DM heterodimerization might not be induced by simple bindings at
301 two sites, but instead mediated by cooperative allosteric conformational changes of the
302 extracellular N-terminal domains and TM domains in both OR molecules. In this case, our
303 description of the dynamic dimer-monomer equilibrium should be considered as a simplified
304 representation of the actual molecular events.
305 To identify the DOR's TMs interacting with MOR, we examined the colocalization of WT-
306 MOR with TM1^{DOR} and TM4^{DOR}, which were previously suggested to interact with TM1^{MOR}.[43,46]
307 TM1^{DOR} and TM4^{DOR} moderately colocalized with MOR when expressed at similar levels (both
308 at densities of 0.5-1.0 fluorescent spots/μm^2; Figure 5B). Furthermore, TM4^{DOR} suppressed DM
309 heterodimerization in an expression level-dependent manner, but not as much as TM1^{MOR}
310 (Figure 5C), indicating its contribution to DM heterodimerization but also suggesting the

311 presence of other significant binding sites, including $TM1^{DOR}$ and other TM domains as well as
312 the N-terminal domain.

313 Despite these findings, we emphasize the critical role played by the interactions of the N-
314 terminal domains of DOR and MOR. This is because the TM interactions are not quite specific,
315 as described. Namely, $TM1^{DOR}$ and $TM4^{DOR}$ are involved in both DM (Figure 3C left) and DK
316 (Figures 2C, left and right, and 2E) heterodimerizations, and $TM1^{MOR}$ is involved in both DM
317 heterodimerization (Figure 3C right; Figure 5D as it blocks DD homodimerization) and MM
318 homodimerization (Figure 5D; also refer to Figures 5B-E in companion paper). In striking
319 contrast, Dpep(20-42)DM had no influence on either MM or DD homodimerization (Figure 5D).
320 A control TM-peptide, TM^{LDLR}, with the sequence of the LDL receptor's TM domain, exhibited
321 no effect on homodimer blocking (Figure 5D).

322 In conclusion, the N-terminal domains of DOR and MOR are specifically involved in DM
323 heterodimerization, whereas the TM domains contribute but interact less specifically: $TM1^{MOR}$
324 in MOR enhances both DM heterodimerization and MM homodimerization, and $TM1^{DOR}$ and
325 $TM4^{DOR}$ in DOR participate in both DM and DK heterodimerization. Meanwhile, DM
326 heterodimerization might involve allosteric interactions between the N-terminal and TM
327 domains.

328

329 **M-agonists' effect on DM heterodimerization**

330 We examined the effects of MOR agonists (M-agonists), morphine and [D-Ala2, N-MePhe4, Gly-
331 ol]-enkephalin (DAMGO), on DM heterodimerization (Figures 6A-6E). At an M-agonist
332 concentration of 0.5 μM in the cell culture medium, MOR would be rapidly bound by morphine
333 and DAMGO (denoted as M^{*mor} and M^{*DAMGO}, respectively),[50] and therefore we examined the
334 M-agonist effect on DM heterodimerization within 5 min after the agonist addition, prior to any
335 detectable internalization. As detailed in the companion paper, DAMGO enhanced MM
336 *homo*dimerization and slightly elongated the MM dimer lifetime (Figures 5C and 5D, respectively,
337 in companion paper).

338 M*^{mor} exhibited almost the same colocalization index with DOR as non-ligated MOR,
339 although the DM*^{mor} heterodimer lifetime was shorter (Figures 6A-6C). The effects of Dpep(20-
340 42) on DM dimerization for M*^{mor} and non-ligated MOR were very similar (Figures 6A, 6B, and
341 6E). M*^{DAMGO} exhibited a greater colocalization index with DOR (DM*^{DAMGO} heterodimers) with
342 a prolonged heterodimer lifetime, compared to MOR in the basal state (Figures 6A-6E). The
343 presence of Dpep(20-42)DM in the medium markedly reduced both the colocalization index and
344 lifetime of the DM*^{DAMGO} heterodimers. The influence of the DOR agonist, 0.5 μM SNC-80, on
345 MOR and SNC-80-bound DOR heterodimerization could not be determined due to the rapid
346 internalization of MOR and DOR after SNC-80 addition, as reported in subsequent sections.
347

348 **Summary of K_D, k_{off}, and k_{on} values and expected percentages of OR protomers**
349 **existing as homo- and hetero-dimers at various expression levels**

350 The equilibrium constants K_Ds were deduced by fitting the experimental PCCF histograms for
351 DM and DK heterodimers with theoretical models (Figure 6A), using hetero-K_D and σ as fitting
352 parameters (Eqs. 26 and 73-75 in Note S2 in companion paper for homodimer). The derived
353 K_D, k_{off}, and k_{on} values for KK, MM, and DD homodimers as well as DM and DK heterodimers,
354 with or without M-agonists and Dpep(20-42)DM, are summarized in Figures 6D and 6E (for the
355 influence of expression levels on the evaluated K_D values with actual curve fitting results, see
356 Figures S4A-S4D; for the SEM, see Tables S2 and S3; all statistical data are summarized in
357 Table S1).

358 Based on the K_D values obtained here, the percentages of OR protomers existing as
359 monomers, DD and MM homodimers, and DM and DK heterodimers in the presence and
360 absence of morphine and DAMGO, at various number densities of ORs expressed in the PM,
361 are calculated and shown in Tables S2-S4 for the cases where DOR and MOR expression levels
362 are equalized. In particular, Table S4 presents the fractions of MOR or DOR protomers existing
363 as monomers, homodimers, and heterodimers. For the cases where expression levels are freely

364 varied, see Figure S5. Without knowing the K_D values for both homo- and hetero-dimerizations,
365 such evaluations would have been impossible.
366
367 **Virtually all OR molecules alternate between existing as homo- and hetero-dimers**
368 **and monomers during short periods on orders of 1-10 s**
369 Cautious interpretations are required for the small percentages of OR protomers, 4.2-21.2%,
370 existing as homo- and hetero-dimers at any moment at low physiological expression conditions
371 (1 copy/μm^2 for each OR; see columns of expression levels of 1 copy/μm^2 and 1+1 copies/μm^2
372 in Tables S2 and S3, respectively; including the presence of morphine and DAMGO, but not
373 peptide dimer blockers). Based on these values, one might consider the functional influence of
374 dimers to be small, but this would be incorrect. Note that the dimer lifetimes are in the range
375 of 118-369 ms, indicating that these dimers fall apart quickly, but then the monomers will again
376 form dimers with different (and sometimes the same) partner molecules (see Figures S2A and
377 S2B in companion paper for an example). This process is continually repeated. Therefore,
378 although at any time the percentages of protomers existing as dimers are limited, virtually all
379 OR molecules rapidly interconvert among homodimer-, monomer-, and heterodimer-states and
380 monomers during short periods on orders of 1-10 s (at physiological expression levels for both
381 molecules) (Figure 6E and Table S3).
382 This indicates that ORs would perform their functions while undergoing rapid monomer-
383 dimer interconversions. If the functionalities of monomers and dimers are different, this raises
384 the possibility to fine-tune the OR functions by modulating monomer-dimer interconversions by
385 natural agonists and synthetic drugs.
386
387 **Lack of morphine-induced internalization of MOR and DOR even in MD cells**
388 Transient DM heterodimerization might affect agonist-induced intracellular signaling and
389 internalizations of MOR and DOR, and thus analgesic efficacy and tolerance development
390 (Figure 7A). Therefore, we examined the effects of DM heterodimerization on downstream

391 signals after M-agonist stimulation and the internalization of MOR and DOR before and after
392 M- and D-agonist stimulation (0.5 μM), using three cell lines produced here: (1) M-cells, CHO-
393 K1 cells stably expressing SNAPf-MOR at 0.5-1.0 fluorescent spots/μm^2 after labeling with
394 SNAP-Surface 549; (2) D-cells, CHO-K1 cells stably expressing SNAPf-DOR at 0.5-1.0
395 fluorescent spots/μm^2 after labeling with SNAP-Surface 549; (3) MD-cells based on M-cells (or
396 D-cells), transiently transfected with the cDNA encoding DOR-Halo (or MOR-Halo), which was
397 labeled with SaraFluor 650T (cells exhibiting 0.5-1.0 fluorescent spots/μm^2 were selected for
398 observations). The two types of MD-cells (based on M-cells or D-cells) are biologically the same
399 (thus, in the following, we simply call them MD-cells), apart from the experimental details (i.e.,
400 for the assay of MOR and DOR internalizations, SNAPf-MOR and SNAPf-DOR must be used,
401 respectively, because our assay depends on the quenching of fluorescence signal from these
402 molecules located on the cell surface using the membrane impermeable quencher; see below
403 and the companion paper). Dpep(20-42)DM (1 μM) was extensively used to dissect the
404 functions of DM heterodimers from those of D/M monomers and DD/MM homodimers.

405 The time courses of OR internalization were monitored for 55 min by measuring the OR
406 molecules remaining in the PM. The OR amounts in the PM were measured by TIRF microscopy,
407 by evaluating the signal intensities of the OR molecules in the TIRF illumination range (in PM
408 plus cytoplasm within ≈100 nm from the PM) before and after the addition of a membrane-
409 impermeable fluorescence quencher, Mn(III) meso-tetra(4-sulfonatophenyl)porphine (Mn^{3+}-
410 TSP) (i.e., the intensity of the fluorescence signal from the cytoplasm in the TIRF illumination
411 range), and then subtracting the latter from the former (see Figures 6A and S6 and related
412 main text in the companion paper; also see STAR Methods). Each time course obtained under
413 various conditions could be fitted with a single exponential function plus a constant. The
414 constant provided the OR fraction whose internalization is undetectable within 55 min, and the
415 exponential decay constant provided the residency lifetime in the PM for the OR's internalized
416 fraction observed during 55 min (Figures 7B and S6; for summaries and statistical test results
417 see Table S5).

418 MOR internalization before and after morphine addition was hardly detectable in either
419 M- or MD-cells (Figure 7B, Left column, Top and middle; Figure S6, Top and third rows). These
420 results indicate that the internalization of DM heterodimers is as slow as that of MOR monomers
421 and homodimers and their internalization rates are not affected by morphine binding. This was
422 further confirmed by the lack of Dpep(20-42)DM effects on M and M^{*mor} internalization (Figure
423 7B, Left column, Top and middle; Figure S6, Top-fourth rows). DOR internalization was similarly
424 unaffected by morphine addition in MD-cells (Figure 7B, Right column, Top and middle; Figure
425 S6, Top-fourth rows).

426 However, these observations require cautious interpretations due to the low fractions of
427 M and M^{*mor} existing as DM and DM^{*mor} heterodimers, respectively, under the employed
428 expression levels (≈5% as shown in Table S3; see the column of 1+1 copies/μm^2; i.e., the case
429 approximating experimental observation conditions of 0.5-1.0 fluorescent spots/μm^2 for both
430 SNAPf-MOR and DOR-Halo), although, as described in the previous subsection, virtually all OR
431 molecules would experience dimer periods within 1-10 s. In certain PM domains in some
432 neurons, the MOR and/or DOR concentrations may far exceed those used in this study (e.g.,
433 MOR in primary cilia),[51] and the morphine effect on the MM and/or DM dimer internalizations
434 could be more pronounced.

435

436 **Highly-enhanced M^{*DAMGO} internalization during transient binding to DOR**

437 In contrast to morphine, DAMGO administration resulted in pronounced internalization of
438 DAMGO-bound MOR (M^{*DAMGO}) in both M- and MD-cells (Figure 7B, Left column, Bottom; Figure
439 S6, Fifth and sixth rows; Table S5). The results in M-cells are virtually the same as those
440 reported in the companion paper (Figure 6B, Middle column and Table 1), which show
441 significant M^{*DAMGO} internalization during 35 min (55 min for the results shown here) that is not
442 influenced by $M^{*DAMGO}M^{*DAMGO}$ homodimerization.

443 In MD-cells, the proportion of internalized M^{*DAMGO} is higher compared to that in M-cells
444 (48% vs. 30%). This difference occurs despite the low fractions of M^{*DAMGO} existing as

445 DM*^{DAMGO} heterodimers (9.1% at time 0) (Table S3; see the 1+1 copies/μm^2 column). The
446 addition of Dpep(20-42)DM to MD-cells, which reduces heterodimeric M*^{DAMGO} from 9.1% to
447 4.3% (Table S3), significantly reduced M*^{DAMGO} internalization from 48% to 26% (Figure 7B
448 and Table S5). Therefore, we conclude that significant M*^{DAMGO} internalization occurs with
449 DM*^{DAMGO} heterodimers in addition to M*^{DAMGO} monomers and homodimers. Although the co-
450 internalization of MOR and DOR following DAMGO exposure has been documented
451 previously,[3,6,52-54] the critical insight obtained here is that DM*^{DAMGO} heterodimers, despite their
452 very low fraction (9.1% of M*^{DAMGO} at low physiological expression levels of ≈1+1 copies/μm^2
453 of MOR and DOR) and short lifetime (369 ± 11 ms; Figures 6C and 6D), contribute to a
454 significant proportion of M*^{DAMGO} internalization.

455 These observations suggest an unanticipated regulatory mechanism for M*^{DAMGO}
456 internalization. Namely, at the moment of DM*^{DAMGO} heterodimer formation, its ability to bind
457 to cellular internalization machineries, such as GRKs and β-arrestin 2,[55] might suddenly rise
458 dramatically, and then the binding affinity would rapidly decline due to DM*^{DAMGO} heterodimer
459 dissociation, which would occur within a fraction of a second ($1/k_{off}$ = 0.37 s; Table S3). Hence,
460 the cycle of DM*^{DAMGO} heterodimerization and dissociation (which occurs every few seconds or
461 so) would function analogously to a car driver adjusting the speed by frequently and briefly
462 pushing on and releasing the gas pedal, to regulate the M*^{DAMGO} internalization rate (Figure
463 7C). Although the enhancement of internalization might occur only during the brief periods
464 when DM*^{DAMGO} heterodimers are formed (Figure 7C), the total frequency of heterodimerization
465 across the PM ensures that the overall internalization of M*^{DAMGO} as DM*^{DAMGO} heterodimers is
466 significant. This correlates with the area under the curve consisting of many short pulses,
467 depicted in Figure 7C.[56-58] Thus, the overall internalization rate of M*^{DAMGO} could be modulated
468 by the frequencies and durations of transient DM*^{DAMGO} heterodimerization events.

469 M*^{DAMGO} monomer/homodimer internalization would occur much less efficiently at the
470 level of individual molecules, but since larger fractions of M*^{DAMGO} exist as monomers at any
471 moment, the overall contributions of M*^{DAMGO} monomers/homodimers to M*^{DAMGO}

472 internalization are quite significant (Figure 7C). If the expression levels of MOR and DOR are
473 elevated in certain cell types, then M^{*DAMGO} internalization would predominantly occur through
474 DM^{*DAMGO} heterodimers.

475 We also examined the effects of the DOR-specific agonist SNC-80 on receptor
476 internalization.[59] The treatment led to extensive internalization of SNC-80-bound DOR (D^{*SNC})
477 in both D- and MD-cells, with similar extents and rates (Figure S7A, middle and right columns;
478 Table S5), indicating that DOR^{*SNC} is internalized without the influence of heterodimerization
479 with MOR. Meanwhile, SNC-80 induced significant MOR internalization in MD-cells, which was
480 reduced by the further addition of Dpep(20-42)DM (Figure S7A, left column; Table S5),
481 indicating that MOR is internalized when it forms heterodimers with D^{*SNC} in MD-cells.

482

483 **Transient DM^{*Ago} heterodimers produce strong short pulse-like signals**

484 We examined the cytoplasmic signals triggered by M-agonists, morphine and DAMGO, by
485 monitoring the intracellular Ca^{2+} mobilization in cells stably expressing Gqi5 and MOR, which
486 were further transiently transfected to express DOR or KOR (called M-, MD-, and MK-cells in
487 this subsection; Figure 7D; cf Figure S1A and STAR Methods as well as the caption to Figure
488 S1A in the companion paper). All ORs were expressed at the same low physiological expression
489 levels employed for single-molecule detection of dimers (0.5-1.0 fluorescent spots/μm^2 for each
490 OR).

491 In M-cells, Ca^{2+} mobilization occurred at comparable intensities upon morphine and
492 DAMGO treatments, without any effect of Dpep(20-42)DM (in the companion paper, which also
493 reports Ca^{2+} mobilization in M-cells, we only used DAMGO as an MOR agonist). No response
494 was evident in D-cells or K-cells (only DAMGO was examined for K-cells). In MD-cells,
495 augmentations of the Ca^{2+} signal compared to that in M-cells were apparent for both morphine
496 and DAMGO (Ca^{2+} signal increase in MD-cells was greater with DAMGO than morphine), which
497 were mitigated by Dpep(20-42)DM. These observations indicate that the overall M^{*Ago}
498 downstream signals (M^{*Ago} denotes agonist-bound MOR, collectively indicating M^{*mor} and

499 M*^{DAMGO}) are greater when DOR is co-expressed. This result is consistent with a previous report
500 indicating that morphine and DAMGO activate MOR with greater efficacy when DOR is co-
501 expressed over MOR alone, but without explicitly estimating the percentages of MOR existing
502 as DM heterodimers.[50]

503 We found very small fractions of M*^{Ago} molecules existing as DM*^{Ago} heterodimers (4.9%
504 for DM*^{mor} and 9.1% for DM*^{DAMGO} at low experimental expression levels of ≈1+1 copies/μm^2
505 in Table S3) for very brief durations (369 ± 11 ms for DM*^{DAMGO} and 187 ± 20 ms for DM*^{mor};
506 Figure 6C). In the case of DAMGO, M*^{DAMGO} molecules existing as a *homo*dimer induce the
507 same signal level as M*^{DAMGO} existing as a monomer (since the presence of FAM-Mpep-TAT or
508 mGFP-Mpep does not affect the Ca^{2+} signal level; Figure 6F in companion paper). These results
509 suggest that the signal production rate (signal induced per unit time) of each M*^{Ago} molecule
510 in a DM*^{Ago} heterodimer must be substantially larger than that of each monomeric or
511 homodimeric M*^{Ago} molecule. This enhanced signaling rate may be induced by conformational
512 changes of M*^{Ago} upon DOR binding and/or those of DOR upon M*^{Ago} binding, which might
513 make a non-ligated DOR signal possible.

514 The enhanced signal from the M*^{Ago} molecules in very limited populations of DM*^{Ago}
515 heterodimers existing for short periods (369 ms) suggests a fundamentally important signaling
516 mechanism by DM*^{Ago} heterodimers, for the same reasons as the enhanced internalization upon
517 DM*^{DAMGO} heterodimerization (previous subsection). Namely, at the moment of DM*^{Ago}
518 heterodimer formation, the probability that the M*^{Ago} molecule and possibly the M*^{Ago}-bound
519 DOR molecule bind to and activate Gqi5 or Gαi, consequently triggering downstream signaling
520 cascades, might rise steeply, but this activation is short-lived because the DM*^{Ago} heterodimer
521 dissociates quickly within fractions of a second ($1/k_{off}$ = 0.19 s and 0.37 s for DM*^{mor} and
522 DM*^{DAMGO}, respectively; Table S3). Hence, a DM*^{Ago} heterodimer will create brief, pulse-like
523 signals, and thus the signal in the entire cell is produced as the sum of the brief, stronger pulse-
524 like signals from individual DM*^{Ago} heterodimers plus the weaker signals from M*^{Ago} monomers
525 (Figure 7C).[56-58] As we proposed previously,[56-58] the regulation of the signal time courses of an

526 entire cell is more readily achieved when signaling entities (individual signaling molecules and
527 molecular complexes) emit short pulse-like signals as opposed to prolonged ones: only simple
528 summation (aggregation) of brief signals suffices to generate the overall cellular signal
529 response, while if individual signals are prolonged, complex integration rather than simple
530 summation must be performed to produce the required cellular signal time courses.[58] In short,
531 the cellular signal intensities might be regulated by adjusting the frequencies of the short pulse-
532 like formation of DM*^{Ago} heterodimers. In addition, in cells with elevated but still physiological
533 OR expression levels, the signals emanating from DM*^{Ago} heterodimers could be quite
534 substantial, governing the cellular signal.
535

536 **Dpep(20-42) reduces morphine tolerance in mice**

537 As described in the previous subsection, Dpep(20-42)DM moderately reduces the M*^{Ago}-
538 induced signal. This effect not only has implications at the cellular level but also might extend
539 to broader physiological contexts, including nervous tissues and systemic functions. Therefore,
540 we examined whether the soluble DM heterodimer blocker peptide Dpep(20-42)DM can
541 modulate morphine-mediated analgesia in murine models. The peptide, dissolved in artificial
542 cerebrospinal fluid (aCSF), was administered directly into the cerebral ventricles at a dose of
543 10 μg/day continuously for two days prior to the commencement of daily subcutaneous
544 morphine injections (10 mg/kg/injection; one injection/day) (Figure 7F). We utilized the tail-
545 flick test to evaluate the analgesic efficacy of morphine and track the progression of
546 antinociceptive tolerance.

547 Our results revealed that the analgesic potency of morphine was enhanced by Dpep(20-
548 42)DM, which was especially evident between 60 and 120 minutes after morphine application
549 over the course of the study (days 1, 5, 8, and 11; Figure S7B). Notably, on day 11, the disparity
550 in analgesic effects between the control aCSF and the peptide groups reached ≈3 fold at the
551 120-minute mark following morphine administration (Figure 7G).

552 Furthermore, the administration of Dpep(20-42)DM reduced the development of morphine
553 tolerance. By day 8 after the morphine treatment was initiated, a noticeable reduction in
554 morphine's analgesic effect was observed in the control group. In contrast, mice treated with
555 the peptide retained ≈80% of the initial antinociceptive efficacy, which was sustained from
556 days 8 to 11 (Figure 7H). These results imply that the inhibition of DM* heterodimerization by
557 Dpep(20-42)DM diminishes the development of antinociceptive tolerance to morphine,
558 suggesting the involvement of crucial neuronal populations within the pain pathway that co-
559 express MOR and DOR, corroborating prior studies.[3,18,21,24] Suppression of DM* heterodimers
560 by Dpep(20-42)DM also diminishes the cellular signal levels (Figure 7E). Accordingly,
561 maintaining proper signal levels in cells might be important for sustained morphine analgesia,
562 which will be discussed further.

563 # Discussion

564 The significance of OR heterodimerization in pain therapy and neuropsychiatric disorders is
565 garnering increasing attention.[7-10] However, our understanding of OR heterodimers and their
566 clinical implications is limited due to the paucity of fundamental knowledge on heterodimer
567 formation dynamics and mechanisms and the lack of specific blockers. Using our advanced
568 single-molecule imaging and analysis methods,[1] we obtained the fundamental parameters K_D,
569 k_{off}, and k_{on}, describing OR homo- and hetero-dimerizations. Crucially, these parameters are
570 independent of OR expression levels, and thus we firmly established the formation of transient
571 DM and DK heterodimers, alongside KK, MM, and DD homodimers, in the PM of cells expressing
572 these molecules. These parameters were determined in the presence and absence of M-
573 agonists and Dpep(20-42)DM (Figure 6E and Tables S2-S3), and the percentages of protomers
574 existing as DM and DK heterodimers at various expression levels were calculated from the K_D
575 values (Tables S3-S4 and Figure S5), which will be useful for future studies to reveal the
576 biological and pharmacological consequences of OR homo- and hetero-dimers. We hardly
577 detected transient OR trimers and tetramers, indicating that at low physiological expression
578 levels, the percentage of OR protomers existing as oligomers greater than dimers would be
579 limited.

580 This study first documented the transient nature of OR heterodimers, revealing lifetimes
581 of DM and DK heterodimers of approximately 250 ms, roughly twice as long as those of
582 homodimers (120 ms for DD and MM and 180 ms for KK). Previous single-molecule imaging
583 studies likely missed the OR dimers due to their scarce presence at the low expression levels
584 typically employed in these studies (≈1 copy/μm^2) and their brief lifetimes.[60-62] Indeed,
585 experiments performed at higher protein densities using bioluminescence resonance energy
586 transfer (BRET), fluorescence resonance energy transfer (FRET), and biochemical assays
587 detected the dimers, although these methods could not elucidate the dynamic nature of OR
588 dimerization.[44,61,63-65] Interestingly, pull-down assays, which require minute-order procedures,

589 detected homo- and hetero-dimers despite their 100-ms-order lifetimes,[18,66] probably due to
590 the rapid reassociation kinetics.

591 The interaction domains critical for heterodimerization have been identified as both the
592 N-terminal domains for DM and both the EL3 domains for DK heterodimers (Figures 2-4). While
593 TM domains contribute to dimerization, they are less specific and primarily augment overall
594 affinity. For example, $TM1^{MOR}$ is involved in MM *homo*dimerization by binding to another MOR
595 (perhaps mainly the TM1 domain), in addition to DM *hetero*dimerization by binding to $TM1^{DOR}$,
596 $TM4^{DOR}$, and other TMs of DOR (Figures 5B-5D). The nature of lower-specificity TM interactions
597 is also found in the literature. The involvement of TM domains in DM heterodimerization[3,46] and
598 DK heterodimerization[31] was previously proposed, whereas the same TM domains such as
599 $TM4^{DOR}$ and $TM1^{MOR}$ were also proposed to be involved in DD[67] and MM[48,68] homodimerizations.
600 As described in the companion paper, specific C-terminal interactions are critical for the
601 formation of KK, MM, and DD homodimers. The TM interactions with lower specificities were
602 previously proposed as the rolling dimer interface model, in which multiple TM interaction sites
603 co-exist and interconvert.[44]

604 Since the addition of either Dpep(20-42)DM (also Mpep(32-61)MD) or $TM1^{MOR}$ alone
605 reduced the colocalization index for DM heterodimers to near-baseline levels (1.2-1.3) (Figures
606 4A, 4B, and 5C), we suggest that DM heterodimerization might also involve cooperative
607 allosteric conformational changes between the N-terminal domains and TM domains in DOR
608 and MOR, which might affect their functions.[69] In addition, although the binding of nucleotide-
609 free Gα to GPCR was proposed to affect GPCR conformations,[70] we did not consider this effect
610 on OR dimerization. The possible involvement of these processes suggests the complexity of
611 OR dimerization, which we have simplified using first-order kinetics to aid our understanding
612 at this stage of research.

613 Our findings also suggest that while TM peptides from ORs will not serve as specific
614 blockers for OR homo- and hetero-dimerizations (Figures 5C and 5D),[3] soluble peptides with
615 sequences mirroring the extracellular heterodimer formation domains ($EL3^{DOR}$ and $EL3^{KOR}$

616 peptides for DK heterodimers and DpepDM and MpepMD for DM heterodimers) can specifically
617 reduce DM and DK *hetero*dimers (Figures 2D, 4, and 5D).

618 We extensively utilized the Dpep(20-42)DM peptide to dissect the functions of M^{*Ago}
619 monomers/homodimers and DM^{*Ago} heterodimers after the application of M-agonists, morphine
620 and DAMGO (where M^{*Ago} collectively denotes agonist-bound MOR). DM^{*Ago} dimerization was
621 enhanced by DAMGO but not morphine, and reduced by Dpep(20-42)DM (Figure 6). Morphine
622 does not induce the internalization of M^{*mor} or DOR even in MD-cells, where DM^{*mor}
623 heterodimerization is induced. M^{*DAMGO} monomers and $M^{*DAMGO}M^{*DAMGO}$ homodimers are
624 internalized in similar manners (Figure 6B in the companion paper), and DM^{*DAMGO}
625 heterodimerization further enhanced M^{*DAMGO} internalization (Figures 7B and 7C). DM^{*Ago}
626 heterodimerization also enhanced the downstream Ca^{2+} signal (Figure 7E). Monomers of a
627 prototypical GPCR, the β2-adrenergic receptor, were previously found to efficiently activate a
628 stimulatory heterotrimeric G protein, Gs,[71] but our results indicate that certain GPCRs, including
629 MOR, might acquire enhanced activities upon heterodimer formation.

630 In our study, conducted under the low physiological receptor expression levels (≈1+1
631 copies/μm^2), only small fractions (≤9.1%) of M^{*Ago} will exist as DM^{*Ago} heterodimers at any
632 moment (Table S3). Combining this with the short 369-ms lifetime of DM^{*Ago} heterodimers, we
633 advanced an argument that each DM^{*Ago} heterodimer will create a brief, intense pulse-like
634 signal, contrasted with the weaker signals from M^{*Ago} monomers, and the overall cellular signal
635 is produced as the sum of these signals (Figure 7C and 7E).[56-58] Note that all M^{*Ago} molecules
636 form DM^{*Ago} heterodimers every 1-10 s even under lower normal physiological expression levels
637 (Figure 6E and Table S3). Enhanced internalization of M^{*DAMGO} might also follow a similar
638 enhancement pattern. These results were observed under expression levels far lower than
639 those typically used in bulk optical and biochemical assays (by factors of 10-1000),[63-65]
640 suggesting a unique signaling mechanism in native physiological conditions.

641 In specific neural tissue domains or certain cell types where OR expression levels are
642 higher,[51] DM^{*Ago} heterodimers could play more dominant role in cellular responses, dictated by

643 the frequency of their transient active phases. Building upon this hypothesis, and recognizing
644 the possibility that small quantities of DM*^{Ago} heterodimers might induce critical signals in key
645 neurons, we explored the *in vivo* effects of Dpep(20-42)DM administered into murine cerebral
646 ventricles to assess its impact on morphine tolerance, unlike a previous study using systemically
647 applied Nterm-TM1^{MOR}-TAT,[3] which would non-specifically block multiple dimer forms (Figure
648 5). We found that cerebral ventricle-administered Dpep(20-42)DM significantly curtails the
649 development of long-term tolerance (Figures 7F-7H). However, directly comparing the
650 effectiveness of Dpep(20-42)DM to Nterm-TM1^{MOR}-TAT is challenging due to differing
651 administration methods and the inherent specificity of Dpep(20-42)DM, which likely contributes
652 to its reduced side effects.

653 Our *in vivo* findings align with previous findings that a genetic or pharmacological
654 blockade of DOR can enhance MOR-agonist induced analgesia, highlighting the role of DM
655 heterodimers in regulating MOR-mediated pain pathways[4,18,21,24,72-74] The newly identified
656 specific extramembrane domains identified for DM heterodimer-blocking present novel targets
657 for modulating OR function, offering strategic avenues for the development of opioid therapies
658 with reduced tolerance and dependence.

659 These *in vivo* results should be compared with our findings in cultured cells, where
660 Dpep(20-42)DM, facilitating DM*^{mor} dissociation into monomers, reduces the Ca^{2+} signal from
661 Gqi5 (Figure 7E). These apparently contrasting findings made *in vivo* and *in vitro* suggest that
662 finely tuning cellular signals upon morphine application is crucial for preventing long-term
663 tolerance in mice. Agents that modulate the levels of DM*^{mor} heterodimers in the PM, like
664 Dpep(20-42)DM, could offer more precise control over drug effects than simply varying
665 morphine dosage.

666

667 **LIMITATIONS OF THE STUDY**

668 We will need to substantiate the pulse-like recruitment of the Gi protein, GRKs, and β-arrestin
669 2 (receptor internalization) to DM*^{Ago} heterodimers, as well as to M*^{Ago} monomers and
670 homodimers, upon M-agonist addition by direct observations. In general, dynamic GPCR
671 heterodimers might be extremely important for delicately tuning the interactions with
672 downstream molecules, including G-proteins, GRKs, and β-arrestins, and thus such studies
673 should be performed with other GPCRs. The pulse-like activations and interactions of
674 molecules, broached by our current research, could be fundamental regulation mechanisms
675 for cellular signaling functions.

676 Furthermore, we will need to comprehensively understand the involvement of the Gi
677 protein, GRKs, and β-arrestin 2, ORs' TM domains, and ORs' possible allosteric conformational
678 changes in ORs' homo- and hetero-dimerizations as well as possible formation of
679 nanodomains of ORs.[75] This will provide a more complete description of the dimerization
680 kinetics and equilibrium. Meanwhile, we believe that the present approach, employing simple
681 first-order kinetics, is useful at this research stage towards a more fundamental
682 understanding of the homo- and hetero-dimerization of ORs as well as those of GPCRs and
683 other membrane molecules in general. The signals after internalization of agonist-bound ORs
684 are not well understood.[76,77] This needs to be addressed.

685 In the present study, we only used morphine, DAMGO, and SNC-80 as agonists. We will
686 need to examine the effects of other agonists in terms of their involvement with homo- and
687 hetero-dimers in OR signaling. More comprehensive testing of the DM and DK
688 heterodimerization blocker peptides for modulating agonist-induced analgesia in murine
689 models will be required.
690

691 **Figure 1. Transient DM and DK heterodimers, but not MK heterodimers, form in the**
692 **PM.**
693 (**A**) Typical image sequence of simultaneous two-color single fluorescent molecule observations
694 and trajectories of the molecules shown in the images. These molecules undergo transient
695 hetero-colocalization and co-diffusion (SNAP-Surface 549-labeled SNAPf-DOR, green;
696 SaraFluor650T-labeled MOR-Halo, magenta).
697 (**B**) DM and DK heterodimers form, but MK heterodimers do not, as detected by colocalization
698 indexes for correct and rotated overlays (see Figures S2C-S2E in the companion paper.[1]
699 Throughout this report, we employ the following conventions. For box plots, horizontal
700 bars, crosses, boxes, and whiskers indicate the median values, mean values, interquartile
701 ranges (25-75%), and 10-90% ranges, respectively; for bar graphs and plots showing mean
702 values, SEM values are provided by bars; and in statistical analyses, * and ns (not significant)
703 indicate $p < 0.05$ and $p \geq 0.05$, respectively, obtained by Tukey's multiple comparison test.
704 The result set used for multiple comparison is indicated by the group of lines in each figure,
705 and different sets are indicated by different colors (e.g., Figures 2C, 3C and 7E). All statistical
706 parameters (number of replicates and *p* values) are summarized in Table S1.
707 (**C**) Summary of K_D and k_{off} values for OR heterodimers.
708 (**D**) Histograms showing the distributions of hetero-colocalization *durations* for correct and
709 rotated overlays. The control histograms for rotated overlays (grey) were fitted by single
710 exponential functions (black), providing the lifetimes of the incidental overlap events between
711 the magenta and green spots (τ_{inci}). The histograms for correct overlays (colors) were fitted by
712 the sum of two exponential functions: The faster decay time (τ_1) was close to the lifetime of
713 incidental overlaps (τ_{inci}), and the slower decay time provided the heterodimer lifetime (τ_2)
714 (Note S1 in the companion paper). The heterodimer lifetime after correction for the trackable
715 duration lifetime is shown in each box. The k_{off} values ($1/\tau_2$) calculated from τ_2 are shown in **C**.
716 (**E**) Comparison of the amino acid sequences among the three classical ORs (rat) in the domains
717 where the amino acid homologies are lower. Asterisks mark the identical amino acids. The
718 entire sequence comparison is given in Figure S4A in the companion paper.

719 **Figure 2. Interaction between EL3 domains of DOR and KOR is involved in DK**
720 **heterodimerization, and DOR's TM1 and TM4 are also involved.**
721 (**A**) The N- and C-terminal domains of DOR and KOR are not involved in DK heterodimerization.
722 DK colocalization indexes of N/C-terminal deletion mutants of DOR and full-length KOR (top)
723 and N/C-terminal deletion mutants of KOR and full-length DOR (bottom).
724 (**B**) Summary of the names and exact amino-acid ranges of the OR domains and TM1-based
725 peptides employed in this work.
726 (**C**) DOR's EL3, TM1, and TM4, but not EL2 and N-term, are involved in DK heterodimerization.
727 (**Left panel**) Because MK heterodimerization scarcely occurs (top), we examined whether MK
728 heterodimerization (MK colocalization index) is enhanced by substituting various MOR domains
729 with the corresponding DOR domains, using WT-KOR as the binding partner (DK
730 heterodimerization as a positive control; second). (**Right panel**) Because DOR binds to KOR
731 to form DK heterodimers (top) and MK heterodimerization rarely occurs (second), we examined
732 whether DK heterodimerization (DK colocalization index) is reduced by substituting various DOR
733 domains with the corresponding MOR domains, using WT-KOR as the binding partner.
734 (**D**) Both EL3 domains of DOR and KOR are involved in DK heterodimerization. Soluble peptides
735 (1 μM) with the aa sequences of the EL3 domains (EL3-domain peptides) of DOR and KOR, but
736 not that of MOR, block DK heterodimerization.
737 (**E**) DOR's TM1 and TM4 bind to KOR. Colocalization indexes show that the affinities to WT-
738 KOR are greater in the order of WT-DOR > DOR's TM1 > DOR's TM4.
739

740 **Figure 3. N-terminal domains of DOR's aa22-42 and MOR's aa32-61, as well as**
741 **DOR's TM1 and TM4 domains, are involved in DM heterodimerization.**
742 (**A**) Involvement of the extracellular N-terminal domains of DOR and MOR in DM
743 heterodimerization, particularly that of DOR's aa22-42 and MOR's aa32-61. The figures show
744 that mutants with various deletions in the N-terminal domains of DOR and MOR exhibit lower
745 colocalization indexes with full-length (WT) MOR and DOR, respectively, compared to the
746 colocalization index between full-length DOR and MOR. At the bottoms of both panels are the
747 results for the C-terminal deletion mutants, indicating the lack of cytoplasmic C-terminal domain
748 involvement in DM heterodimerization.
749 (**B**) Histograms showing the colocalization *duration* distributions for the pair of WT-MOR and
750 DOR(Δ22-42) (**left**, blue) and the pair of WT-DOR and MOR(Δ32-61) (**right**, magenta).
751 Histograms for the control and rotated overlays of WT DOR-MOR images are the same as those
752 shown in **Figure 1D.**
753 (**C**) The extracellular N-terminal domains of DOR and MOR are involved in DM
754 heterodimerization (left and right panels, respectively), as are DOR's TM1 and TM4 domains,
755 but not the TM6 domain (left panel). (**Left panel**) Based on the finding that MK
756 heterodimerization hardly occurs, we examined whether the DM colocalization index is reduced
757 upon substitutions of DOR domains with the corresponding KOR domains, using WT-MOR as
758 the partner. (**Right panel**) The DM colocalization index is reduced upon the substitution of
759 MOR's N-terminal domain with KOR's N-terminal domain, which is not involved in DK
760 heterodimerization (Figure 2A), indicating the involvement of MOR's N-terminal domain in DM
761 heterodimerization.
762

763 **Figure 4. Soluble Dpep(20-42)DM and Mpep(32-61)DM peptides suppress DM**
764 **heterodimerization.**
765 (**A**) Effect of the addition of 1 μM soluble peptides with the same amino-acid sequences as
766 various parts of the N-terminal domains of DOR and MOR (DpepDM and MpepDM, respectively)
767 on the DM colocalization index.
768 (**B**) With an increase of the Dpep(20-42)DM concentration, the DM colocalization index
769 decreased. The grey keys at 0 μM Dpep(20-42)DM represent the data points obtained by using
770 rotated overlays.
771 (**C**) Dpep(20-42)DM reduces the τ_2 of DM colocalization (blue). Histograms for the control (no
772 addition) and rotated overlays of WT DOR-MOR images are the same as those shown in **Figure**
773 **1D.**
774

775 **Figure 5. $TM1^{MOR}$ interacts with DOR and blocks DM heterodimers, and additionally**
776 **inhibits MM and DD homodimers, whereas Dpep(20-42)DM only blocks DM**
777 **heterodimer formation.**
778 (**A**) Experimental design for examining the interactions of $TM1^{MOR}$, Nterm-$TM1^{MOR}$, and $TM4^{DOR}$
779 (Figure 2B) with WT-ORs (top). For the correct orientation of $TM4^{DOR}$ in the PM, it was linked
780 to the transmembrane domain of LDL receptor (TM^{LDLR}).[78] Representative single-molecule
781 images of DOR-mGFP (green), MOR-Halo (magenta), and SNAPf-$TM1^{MOR}$ (cyan) co-expressed
782 at similar levels of 0.5-1.0 fluorescent spots/μm^2 (bottom).
783 (**B**) $TM1^{MOR}$ and Nterm-$TM1^{MOR}$ form dimers with WT-DOR as efficiently as WT-MOR does.
784 $TM1^{DOR}$ and $TM4^{DOR}$ form dimers with WT-MOR to lesser extents. Expression levels of all
785 molecules were adjusted to 0.5-1.0 fluorescent spots/μm^2.
786 (**C**) Reduction of the DM colocalization index with an increase in the number densities of the
787 TM peptides ($TM1^{MOR}$, Nterm-$TM1^{MOR}$, and $TM4^{DOR}$) relative to that of MOR, expressed in the
788 PM. DOR and MOR were both expressed at levels of 0.5-1.0 fluorescent spots/μm^2. The effects
789 of $TM1^{MOR}$ and Nterm-$TM1^{MOR}$ are stronger than that of $TM4^{DOR}$. The rectangular box without
790 the peptides (x = 0) indicates the result of the box plot without datapoints (to avoid excessive
791 complexity in the plot).
792 (**D**) $TM1^{MOR}$ and Nterm-$TM1^{MOR}$ reduce MM and DD homodimers (in addition to DM
793 heterodimers), but 1 μM Dpep(20-42)DM does not. $TM1^{MOR}$ and Nterm-$TM1^{MOR}$ expression
794 levels were ≈10x of MOR and DOR, following the results shown in panel **C**. TM^{LDLR} is a
795 negative control, representing non-interacting TM domains.
796

797 **Figure 6. Effects of M-agonists, morphine and DAMGO, on DM heterodimerization,**
798 **and of Dpep(20-42)DM on DM heterodimerization, in the presence of M-agonists.**
799 (**A**) Experimental PCCFs for DM heterodimerization in the presence and absence of 0.5 μM M-
800 agonists and 1 μM Dpep(20-42)DM and their fitting curves using K_D for DM heterodimerization
801 and σ (precisions of single-molecule localizations for the two probes and spatial precision for
802 overlaying two-color images) as fitting parameters. MD-cells expressing both DOR and MOR at
803 0.5-1.0 fluorescent spots/μm^2 were employed.
804 (**B**) Colocalization indexes obtained from the PCCFs shown in **A**. Together with the results
805 shown in **A**, the results indicate that morphine hardly affects DM heterodimerization whereas
806 DMAGO enhances it. The Dpep(20-42)DM addition significantly reduces DM heterodimers under
807 all conditions examined here.
808 (**C**) Morphine shortens and DAMGO prolongs DM heterodimer lifetimes, whereas the further
809 addition of Dpep(20-42)DM reduces the lifetimes, making them shorter than those for DM
810 heterodimers without any treatment.
811 (**D**) Schematic summary of K_D and k_{off} values for DM heterodimers in the presence and
812 absence of DAMGO and DpepDM(20-42)DM.
813 (**E**) Summary of K_D, k_{off}, and k_{on} values for OR homodimers and DM and DK heterodimers,
814 including the cases in the presence and absence of morphine or DAMGO and DpepDM(20-
815 42)DM (DpepEL3 in the case of DK heterodimers), wherever appropriate.
816

817 **Figure 7. Dpep(20-42)DM helps to dissect the DM heterodimer and MOR monomer**
818 **functions after M-agonist applications in cells, and enhances morphine analgesia**
819 **and reduces tolerance development in mice.**
820 (**A**) Schematic figure showing that Dpep(20-42)DM reduces DM heterodimers, helping to
821 dissect the DM heterodimer and MOR monomer functions, including signaling and
822 internalization, upon M-agonist addition.
823 (**B**) Time courses of MOR and DOR internalization (left and right columns, respectively) before
824 and after the addition of 0.5 μM morphine or DAMGO (top, middle, and bottom boxes,
825 respectively) in the presence and absence of 1 μM DpepDM. MOR internalization was examined
826 in MD-cells and M-cells, whereas DOR internalization was observed only in MD-cells (MOR and
827 DOR internalizations upon D-agonist addition were observed in MD-cells and D-cells, see Figure
828 S7A). The fitting results for these time courses are not depicted here for clarity, but are shown
829 in Figure S6.
830 (**C**) Schematic illustration showing immensely enhanced efficiencies of binding to internalization
831 machineries such as GRKs and β-arrestins and of DM*^{DAMGO} heterodimer internalization,
832 occurring in the brief lifetimes of DM*^{DAMGO} heterodimers. M*^{DAMGO} monomers' internalization
833 efficiency is low, but due to the presence of many M*^{DAMGO} monomers, they are responsible for
834 the internalization of half of the M*^{DAMGO} molecules in the PM.
835 (**D**) (**Top**) Experimental design for observing Ca^{2+} mobilization after M-agonist addition. Ca^{2+}
836 mobilization was monitored by Fluo-4 fluorescence intensity in M-, D-, and MD-cells. (**Bottom**)
837 Fluo-4 images and single-molecule images of DOR and MOR. Ca^{2+} mobilization was
838 parametrized by using $[F_{Max}-F_b]/F_b$, where F_{Max} is the maximal Fluo-4 signal intensity within 75
839 s after stimulant addition and F_b is the baseline intensity (insert in Figure D).
840 (**E**) Ca^{2+} mobilization parametrized by using $[F_{Max}-F_b]/F_b$ for Fluo-4 signals before and after the
841 addition of morphine and DAMGO, in the presence and absence of Dpep(20-42)DM.
842 (**F**) Schematic illustration showing the osmotic pump implantation for intracerebroventricular
843 injection of Dpep(20-42)DM and subcutaneous morphine injection in mouse.

844 (**G**) Tail flick test results on day 11, showing that morphine-induced analgesia was enhanced
845 by the continuous administration of Dpep(20-42)DM (10 μg/day). The enhancing effect lasted
846 for at least 120 min.
847 (**H**) Tolerance to morphine was demonstrated by the loss of the analgesic response from day
848 8, reduced to ≈50% of the initial efficacy on day 11 in the control aCSF-treated mice (AUC =
849 area under the antinociception vs. time curves shown in Figure S7B). In contrast, the
850 antinociceptive effect of morphine in DpepDM-treated mice was maintained at ≈80% of the
851 initial efficacy on days 8 and 11. All experiments were randomized and performed by a blinded
852 researcher, who was then unblinded before statistical analysis.
853

854 **STAR METHODS**

855 Detailed methods are provided in the online version of this paper and include the following:

856

857 KEY RESOURCES TABLE

858 RESOURCE AVAILABILITY

859 Lead contact

860 Materials availability

861 Data and code availability

862 EXPERIMENTAL MODEL AND SUBJECT DETAILS

863 Cell lines and culture

864 Mice

865 Plasmids and cloning

866 METHOD DETAILS

867 Transfections

868 Microscope observations

869 Fluorescence labeling of ORs

870 Single fluorescent-molecule imaging

871 Evaluating colocalization durations

872 Evaluating the colocalization index

873 Monte-Carlo simulations

874 Cell treatments with agonists and peptides

875 Ca^{2+} mobilization assay

876 Quantifying the internalization of SNAPf-ORs

877 Systemic morphine administration to mice and examination of its antinociceptive effect

878 Intracerebroventricular administration of the Dpep(20-42)DM peptide in mice

879 Morphine-induced antinociception assay

880 QUANTIFICATION AND STATISTICAL ANALYSIS

Statistical analysis

SUPPLEMENTAL INFORMATION

Supplemental information can be found online at ……

ACKNOWLEDGMENTS

We thank Profs. H. Takeshima of Kyoto University, R. Schülz of the University of Münich, and R. Y. Tsien of the University of California San Diego, for their kind gifts of cDNAs encoding rat KOR and DOR, that encoding rat MOR, and that encoding mCherry, respectively. We also thank Ms. Irina Meshcheryakova for technical help in preparing the cDNAs. This work was supported in part by Japan Society for the Promotion of Science (JSPS) Grants-in-Aid for Scientific Research (Kiban A to A.K. [21H04772], Kiban S to A.K. [16H06386], Kiban B to T.K.F. [16H04775, 20H02585], Kiban C to R.S.K. [17K07333], Wakate B to R.S.K. [26870292], Wakate to T.A.T. [21K15058], and Challenging Exploratory Research to T.K.F. [18K19001] and A.K. [22K19334]), a Grant-in-Aid from the Ministry of Education, Culture, Sports, Science and Technology of Japan (MEXT) for Transformative Research Areas (A) to T.K.F. (21H05252), and a JST grant ACT-X to T.A.T. (JPMJAX211B). WPI-iCeMS of Kyoto University is supported by the World Premiere Research Center Initiative (WPI) of MEXT.

AUTHOR CONTRIBUTIONS

P.Z., R.S.K., and A.K. conceived and formulated the project. A.K., T.A.T., T.K.F., and P.Z. developed the simultaneous dual-color single-molecule tracking station. P.Z. and A.K. designed biological experiments, and P.Z., with help from T.A.T., performed virtually all of the microscopic experiments. T.K.F., T.A.T., and A.K. developed and improved the in-house image analysis software and instrument control software, and discussed single-molecule imaging data. S.P. developed the theory for evaluating the dimer lifetimes from the single-molecule experimental data and assisted with its application to experimental results. T.A.T. and P.Z.

908 analyzed the PCCF histograms and obtained dimer dissociation constants. W.F., with help from
909 H.U., performed mouse experiments. P.Z., A.K., and T.A.T. wrote the manuscript, and all
910 authors discussed the results and participated in the manuscript revisions.

911

912 ## DECLARATION OF INTERESTS

913 PZ and AK have a patent pending for DpepDMs, MpepMDs and peptides from EL3 domains of
914 ORs. The remaining authors have no conflicts of interest to declare.

915

916 # STAR Methods

917 ## Key resources table

REAGENT or RESOURCE	SOURCE	IDENTIFIER
Bacterial and virus strains		
E. coli HST08 Premium Competent Cells	Takara	Cat# 9128
Chemicals, peptides, and recombinant proteins		
Morphine hydrochloride	Takeda Pharmaceutical Co., Ltd.	Cat# T8-00705
DAMGO	Sigma-Aldrich	Cat# E7384
SNC-80	Sigma-Aldrich	Cat# S2812
Mn (III) meso-tetra(4-sulfonatophenyl)porphine chloride Mn^{3+}-TSP	Frontier Scientific	Cat# MnT1239
Medetomidine Hydrochloride (Dorbene vet ®)	Kyoritsu Seiyaku Corp., Tokyo, Japan	Cat# 4992945117478 (JAN code)
Midazolam (SANDOZ®)	Sandoz K.K., Tokyo, Japan	Cat# 4987614243022 (JAN code)
Butorphanol tartrate (Vetorphale®)	Meiji Seika Pharma, Tokyo, Japan	Cat# 222866132 (JAN code)
Povidone-Iodine	Meiji Seika Pharma, Tokyo, Japan	Cat# 25655-41-8
Atipamezole Hydrochloride (Atipame®)	Kyoritsu Seiyaku Corp., Tokyo, Japan	Cat# 4992945117461 (JAN code)
DpepDM	Cosmo-Bio	N/A
MpepMD	Cosmo-Bio	N/A
$EL3pep^{DOR}$	Cosmo-Bio	N/A
$EL3pep^{KOR}$	Cosmo-Bio	N/A
SNAP-Surface 549 linker	New England Biolabs	Cat# S9112S
SaraFluor650T Halo ligand	Goryo Chemical	Cat# A308-02
Critical commercial assays		
Gibson Assembly Master Mix	New England BioLabs	Cat# E2611L
Mycoplasma PCR Detection Kit	Beyotime Biotechnology	Cat# C0301S
VenorGeM Mycoplasma Detection Kit	Minerva Biolabs	Cat# MNV11-1100
SF Cell Line 4D-Nucleofector X Kit L	Lonza	Cat# V4XC-2012
Fluo 4-AM special packaging	Dojindo	Cat# F312
Rhod-3 Calcium Imaging Kit	Thermo Fisher Scientific	Cat# R10145
Experimental models: Cell line and mouse line		
Chinese Hamster: CHO-K1	Dainippon Pharma Co., Ltd.	Cat# 03-402
Mice C57BL/6N mice	CLEA Japan, Inc., Tokyo, Japan	Cat# C57BL/6NJcl
Recombinant DNA		
Plasmid: pEGFP	Clontech	Cat# Z2370N
Plasmid: pmCherry	Clontech	Cat# Z2522N
Plasmid: pPBpuro	Michiyuki Matsuda (Kyoto University)[79]	N/A
Plasmid: pCMV-mPBase	Michiyuki Matsuda (Kyoto University)[79]	N/A
SNAPf	New England Biolabs	Cat# N9172S
Halo7	Promega	Cat# G9651
mEGFP	Clontech	Cat# Z2370N

mCherry	Roger Y. Tsien (University of California San Diego)[80]	N/A
CD47	Eric C Brown (Genentech) [81]	N/A
CD28	Simon J Davis (University of Oxford)[82]	N/A
TM^{LDLR}	[78]	N/A
rat KOR	Hiroshi Takeshima (Kyoto University)[83]	N/A
rat MOR-GFP	Rüdiger Schulz (University of Munich)[84]	N/A
rat DOR	Hiroshi Takeshima (Kyoto University)[83]	N/A
GNA15	OriGene	Cat#: SC125360
SNAPf-$TM1^{DOR}$	This paper	N/A
TM^{LDLR}-$TM4^{DOR}$-SNAPf	This paper	N/A
SNAPf-$TM1^{MOR}$	This paper	N/A
SNAPf-Nterm-$TM1^{MOR}$	This paper	N/A
SNAPf-TM^{LDLR}	This paper	N/A
Software and algorithms		
HSR v2.3.1.0	Hamamatsu Photonics	https://www.hamamatsu.com/jp/en.html
MCR v1.2.0.0	Hamamatsu Photonics	N/A
PFV v3.6.6.0	Photron	https://www.photron.co.jp
LabVIEW 2018 v18.0.1f4	National Instruments	RRID:SCR_014325 (https://www.ni.com/en-us.html)
MatLab 2019a v9.6.0	MathWorks	RRID:SCR_001622 (https://www.mathworks.com)
ImageJ (Fiji) v2.1.0	[85]	RRID:SCR_002285 (https://imagej.net/software/fiji/)
Photoshop CC 2021 v22.4.2	Adobe	RRID:SCR_014199 (https://www.adobe.com)
Illustrator CC 2021 v.24.3	Adobe	RRID:SCR_010279 (https://www.adobe.com)
Origin 2017 v.b9.490.220	Origin Lab	RRID:SCR_014212 (https://www.originlab.com)
R studio v1.2.1335	R studio	RRID:SCR_000432 (https://www.rstudio.com)
Excel v16.51	Microsoft	https://www.microsoft.com/en-us/microsoft-365/excel

RESOURCE AVAILABILITY

Lead contact

Further information and requests for resources and reagents should be directed to and will be fulfilled by the lead contact.

Materials availability

Plasmids and cell lines generated in this study will be shared by the lead contact upon request.

Data and code availability

All data generated or analyzed for this study are available within the paper and its associated Supplementary Information. Any additional information required to reanalyze the data reported in this paper is available from the lead contact upon reasonable request. Superimpositions of image sequences obtained in two colors and tracking single-molecules for *in vitro* observation data were performed using C++-based computer programs, produced in-house[86] and based on well-established approaches. Source codes for this have been integrated into a large, complex software package. While the software package cannot be extracted in a useful way, the entire software package is available from the lead contact upon reasonable request, who will provide guidance on how to use it, as its manual and comments are written in Japanese.

EXPERIMENTAL MODEL AND SUBJECT DETAILS

Cell lines and culture

See the companion paper[1] under the same title.

Mice

Male C57BL/6N mice (30-40 g) were purchased from CLEA Japan, Inc. and maintained on a 12-h light/dark cycle with rodent chow and water available ad libitum. They were housed in groups of four until testing. Animal studies were performed according to protocols approved by the Nagasaki University Animal Care and Use Committee (Approved number: 2002181596).

Plasmids and cloning

See the companion paper under the same title.

METHOD DETAILS

Transfections

See the companion paper under the same title.

955

956 **Microscope observations**

957 See the companion paper under the same title.

958

959 **Fluorescence labeling of ORs**

960 The SNAPf-tag-protein fused to ORs was fluorescently labeled with the SNAP-Surface 549 ligand,
961 basically as described in the companion paper.[1] The Halo7-tag protein fused to the intracellular C-
962 terminus of the OR (Figure S1A) was covalently conjugated with SaraFluor650T-Halo-ligand (Goryo
963 Kayaku), by incubating the cells with 100 nM Halo ligand. The SNAPf-OR and OR-Halo7 proteins were
964 simultaneously labeled in the growth medium, at 37˚C in the CO_2 incubator for 30 min. The cells were
965 washed three times with fresh medium (5-min incubation each time), and then the Ham's F12
966 observation medium was added.

967 The labeling efficiency was determined by using the SNAPf-CD47-mGFP and mGFP-CD47-Halo7
968 proteins expressed in the PM (Figure S1C). CD47 is a monomeric 5-pass transmembrane protein
969 expressed in the PM.[87] We could not use ORs for this purpose because they form transient dimers,
970 and thus employed monomeric CD47. For further details, refer to STAR Methods and Figures S1C-E in
971 the companion paper.[1]

972 The fluorescence labeling efficiencies under our normal conditions were 60% and 88% for SNAP-
973 Surface 549 and SaraFluor650T, respectively (Figure S1C). By controlling the expression levels and
974 using these labeling conditions, the spot numbers of SNAPf-OR and OR-Halo7 proteins were
975 approximately equalized (0.75 ± 0.25 spots/μm^2 for each color; i.e., a total spot number density of 1.5
976 ± 0.5 spots/μm^2).

977

978 **Single fluorescent-molecule imaging**

979 Fluorescently labeled ORs expressed in the bottom PM (the PM facing the coverslip) at fluorescent-
980 spot number densities of 0.75 ± 0.25 spots/μm^2 for each color (a total spot number density of 1.5 ±
981 0.5 spots/μm^2) were observed at the level of single molecules at 37˚C, using a home-built objective
982 lens-type TIRF microscope constructed on an inverted microscope (Olympus IX-83)[88-90] (see the
983 companion paper for details). ORs tagged with fluorescent probes were excited with TIR illumination
984 using the following power densities: SNAP-Surface 549 at 561 nm (Coherent OBIS 561-100 LS) at 0.35
985 $\mu W/\mu m^2$; and SaraFluor650T at 642 nm (Omicron LuxXPlus 640-140) at 0.50 $\mu W/\mu m^2$. Simultaneous
986 two-color single-molecule imaging and analysis were conducted as described in the companion
987 paper.[90]

988

989 **Evaluating colocalization durations**

990 See the companion paper under the same title. The trackable duration lifetime (τ_{track}) for SNAP-
991 Surface 549 bound to SNAPf-MOR was 16.3 ± 1.2 s (n = 500; the same as those described in the
992 companion paper)and that for SaraFluor650T-Halo-ligand bound to MOR-Halo was 12.5 ± 0.8 s (n =
993 500) (expressed in CHO-K1 cells) (Figure S1F).
994
995 **Evaluating the colocalization index**
996 See the companion paper under the same title.
997
998 **Monte-Carlo simulations**
999 See the companion paper under the same title.
1000
1001 **Cell treatments with agonists and peptides**
1002 M-agonists, DAMGO (Sigma-Aldrich) and morphine (Takeda), and D-agonist SNC-80 (Sigma-Aldrich)
1003 were applied to the cells as described in the companion paper. DpepDM and MpepMD peptides,
1004 custom-synthesized by Cosmo-Bio, are soluble peptides, and were dissolved in the observation
1005 medium and added to the cells in the observation medium at a selected final peptide concentration at
1006 37˚C. Since their target sites are located on the cell surface, the complex procedures employed for
1007 incorporating the FAM-Xpep-TATs inside the cells, as described in the companion paper, were
1008 unnecessary.
1009
1010 **Ca^{2+} mobilization assay**
1011 The Ca^{2+} mobilization assay was performed in basically the same way as described in the companion
1012 paper. However, when we observed Ca^{2+} responses using the cells expressing SNAPf-MOR, we
1013 employed the CHO-K1 cells stably expressing both Gqi5 and SNAPf-MOR (at number densities of 0.75
1014 ± 0.25 spots/μm^2 when labeled with SNAP-Surface549). To observe the effect of DOR-Halo and KOR-
1015 Halo co-expression, the cells stably expressing Gqi5 and SNAPf-MOR were transiently transfected with
1016 the cDNAs encoding these proteins. The cells exhibiting spot densities of DOR-Halo or KOR-Halo at
1017 0.75 ± 0.25 spots/μm^2 (after labeling with Halo-SaraFluor650T) were selected for observations.
1018 Therefore, the Ca^{2+} mobilization assay was performed at about the same low expression levels of ORs
1019 as those employed for single fluorescent-molecule imaging experiments.
1020
1021 **Quantifying the internalization of SNAPf-ORs**
1022 See the companion paper under the same title.
1023
1024 **Systemic morphine administration to mice and examination of its antinociceptive effect**

1025 Morphine hydrochloride (Takeda Pharmaceutical) was dissolved in saline and subcutaneously
1026 administered to mice once each day (10 mg/kg) for 11 days. Antinociception was measured by the
1027 tail-flick test on days 1, 5, 8, and 11 from 0 to 120 min after morphine administration (details will be
1028 described later). Body weight was measured before each morphine injection. The control group
1029 received saline without morphine. All animal experiments were randomized and performed by a
1030 blinded researcher, who was then unblinded before statistical analysis.
1031

1032 **Intracerebroventricular administration of the Dpep(20-42)DM peptide in mice**

1033 The Dpep(20-42)DM peptide was dissolved in freshly prepared aCSF (127 mM NaCl, 1.5 mM KCl, 1.24
1034 mM KH_2PO4, 1.4 mM $MgSO_4$, 26 mM $NaHCO_3$, 2.4 mM $CaCl_2$, 10 mM D-glucose). For continuous
1035 intracerebroventricular administration, an osmotic minipump (Alzet model 2002) filled with the
1036 peptide solution was implanted according to the manufacturer's protocol and as described
1037 previously.[91] In order to stabilize the pump flow rate, the pumps were primed by placing them in
1038 sterile saline at room temperature overnight. The osmotic minipumps were filled with 200 µL of aCSF
1039 with or without the peptide solution (0.83 mg/mL in aCSF). The minipump was connected to a 2.5-
1040 mm-long cannula (Alzet Brain Infusion Kit 3) via a 1.5-cm-long polyvinylchloride tube. Before surgery,
1041 the mice were anesthetized with a combination anesthetic (0.75 mg/kg of medetomidine, 4.0 mg/kg
1042 of midazolam, and 5.0 mg/kg of butorphanol). The scalp was shaved, Povidone-Iodine (Isodine,
1043 Mundipharma K.K.) was applied, and an incision was made along the midline of the scalp; hemostats
1044 were then used to make a pocket under the skin between the shoulder blades. The skull was scraped
1045 clean of periosteum so that the cannula can properly adhere to the skull. A microdrill (Tamiya, Inc.)
1046 was used to create a hole approximately 1.1 mm lateral and 0.5 mm caudal to the bregma. The
1047 minipump was placed in the pocket under the skin between the shoulder blades, the cannula was
1048 inserted through the drilled hole into the lateral ventricle, and the cannula pedestal was affixed to the
1049 skull with cyanoacrylate glue and resin cement. The incision was closed with soft silk sutures and
1050 antibacterial ointment was applied to the wound. The animals were allowed to rest on a disposable
1051 heating pad until they were recovered by using 0.75 mg/kg of atipamezole and then returned to their
1052 home cages in the animal facility for 1-2 days until the measurement. Cannula placement into the
1053 lateral ventricle was verified with trypan blue (4%, 10 µl).
1054

1055 **Morphine-induced antinociception assay**

1056 Morphine-induced antinociception was evaluated by using the tail-flick test.[22] Using a tail-flick
1057 apparatus (IITC Life Science), the intensity of the heat source was set at 10, which resulted in a basal
1058 tail-flick latency of 2-3 s for most of the animals. The tail-flick latency was recorded before (0 min,
1059 baseline latency) and every 30 min after morphine injection (30, 60, 90, and 120 min). The results are

1060 presented as a percentage of the maximal possible effect, %MPE, which was calculated for each
1061 mouse at each time point according to the following formula: %MPE = [(latency after drug − baseline
1062 latency)/ (10 − baseline latency)] × 100. Cutoff latency was selected at 10 s to minimize tissue
1063 damage. The area under the %MPE vs. time curve (AUC) for each treatment condition was also used
1064 to evaluate antinociception (Figure 7H). Normal distribution of the data was verified before
1065 performing the parametric statistical analysis. Wherever appropriate, data were analyzed using two-
1066 way ANOVA, followed by Tukey's post hoc tests or a multiple unpaired t-test with significance set at P
1067 < 0.05. All calculations were performed using the GraphPad Prism 9 software (GraphPad Software).
1068

1069 ## QUANTIFICATION AND STATISTICAL ANALYSIS

1070 The same as described in the companion paper.[1]

1071

REFERENCES

1. Zhou, P., Tsunoyama, T.A., Kasai, R.S., Hirosawa, K.M., Kalay, Z., Aladag, A., Fujiwara, T.K., Pigolotti, S., and Kusumi, A. (2024). Single-molecule detection of transient dimerization of opioid receptors 1: Homodimers' effect on signaling and internalization. Companion paper.
2. Fujita, W., Gomes, I., and Devi, L.A. (2014). Revolution in GPCR signalling: opioid receptor heteromers as novel therapeutic targets: IUPHAR review 10. Br. J. Pharmacol. *171*, 4155-4176.
3. He, S.Q., Zhang, Z.N., Guan, J.S., Liu, H.R., Zhao, B., Wang, H.B., Li, Q., Yang, H., Luo, J., Li, Z.Y.*, et al.* (2011). Facilitation of μ-opioid receptor activity by preventing δ-Opioid receptor-mediated codegradation. Neuron *69*, 120-131.
4. Keresztes, A., Olson, K., Nguyen, P., Lopez-Pier, M.A., Hecksel, R., Barker, N.K., Liu, Z., Hruby, V., Konhilas, J., Langlais, P.R., and Streicher, J.M. (2022). Antagonism of the mu-delta opioid receptor heterodimer enhances opioid antinociception by activating Src and calcium/calmodulin-dependent protein kinase II signaling. Pain *163*, 146-158.
5. Möller, J., Isbilir, A., Sungkaworn, T., Osberg, B., Karathanasis, C., Sunkara, V., Grushevskyi, E.O., Bock, A., Annibale, P., Heilemann, M.*, et al.* (2020). Single-molecule analysis reveals agonist-specific dimer formation of μ-opioid receptors. Nat. Chem. Biol. *16*, 946-954.
6. Milan-Lobo, L., and Whistler, J. (2011). Heteromerization of the μ- and δ-opioid receptors produces ligand-biased antagonism and alters μ-receptor trafficking. J. Pharmacol. Exp. Ther. *337*(3) 868-75.
7. Szafran, K., Faron-Górecka, A., Kolasa, M., Kuśmider, M., Solich, J., Żurawek, D., and Dziedzicka-Wasylewska, M. (2013). Potential role of G protein-coupled receptor (GPCR) heterodimerization in neuropsychiatric disorders: a focus on depression. Pharmacol. Rep. *65*, 1498-1505.
8. Fribourg, M., Moreno, J.L., Holloway, T., Provasi, D., Baki, L., Mahajan, R., Park, G., Adney, S.K., Hatcher, C., Eltit, J.M.*, et al.* (2011). Decoding the signaling of a GPCR heteromeric complex reveals a unifying mechanism of action of antipsychotic drugs. Cell *147*, 1011-1023.
9. Kabli, N., Nguyen, T., Balboni, G., O'Dowd, B.F., and George, S.R. (2014). Antidepressant-like and anxiolytic-like effects following activation of the μ-δ opioid receptor heteromer in the nucleus accumbens. Mol. Psychiatry *19*, 986-994.
10. Valentino, R.J., and Volkow, N.D. (2018). Untangling the complexity of opioid receptor function. Neuropsychopharmacology *43*, 2514-2520.
11. Levac, B.A.R., O'Dowd, B.F., and George, S.R. (2002). Oligomerization of opioid receptors: generation of novel signaling units. Curr. Opin. Pharmacol. *2*, 76-81.

1110 12. Schmid, C.L., Kennedy, N.M., Ross, N.C., Lovell, K.M., Yue, Z., Morgenweck, J., Cameron,
1111 M.D., Bannister, T.D., and Bohn, L.M. (2017). Bias factor and therapeutic window
1112 correlate to predict safer opioid analgesics. Cell *171*, 1165-1175.e1113.
1113 13. Darcq, E., and Kieffer, B.L. (2018). Opioid receptors: drivers to addiction? Nat. Rev.
1114 Neurosci. *19*, 499-514.
1115 14. Chan, H.C.S., McCarthy, D., Li, J., Palczewski, K., and Yuan, S. (2017). Designing safer
1116 analgesics via μ-opioid receptor pathways. Trends Pharmacol. Sci. *38*, 1016-1037.
1117 15. Cong, X., Maurel, D., Déméné, H., Vasiliauskaité-Brooks, I., Hagelberger, J., Peysson,
1118 F., Saint-Paul, J., Golebiowski, J., Granier, S., and Sounier, R. (2021). Molecular insights
1119 into the biased signaling mechanism of the μ-opioid receptor. Mol. Cell *81*, 4165-4175.
1120 e4166.
1121 16. Ferré, S., Casadó, V., Devi, L.A., Filizola, M., Jockers, R., Lohse, M.J., Milligan, G., Pin, J.-
1122 P., and Guitart, X. (2014). G protein–coupled receptor oligomerization revisited:
1123 functional and pharmacological perspectives. Pharmacol. Rev. *66*, 413.
1124 17. Pan, Z.Z. (1998). μ-Opposing actions of the κ-opioid receptor. Trends Pharmacol. Sci. *19*,
1125 94-98.
1126 18. Gomes, I., Gupta, A., Filipovska, J., Szeto, H.H., Pintar, J.E., and Devi, L.A. (2004). A role
1127 for heterodimerization of μ and δ opiate receptors in enhancing morphine analgesia.
1128 Proc. Natl. Acad. Sci. U.S.A. *101*, 5135-5139.
1129 19. Gupta, A., Mulder, J., Gomes, I., Rozenfeld, R., Bushlin, I., Ong, E., Lim, M., Maillet, E.,
1130 Junek, M., Cahill, C.M.*, et al.* (2010). Increased abundance of opioid receptor heteromers
1131 after chronic morphine administration. Sci. Signal. *3*, ra54-ra54.
1132 20. Olson, K.M., Keresztes, A., Tashiro, J.K., Daconta, L.V., Hruby, V.J., and Streicher, J.M.
1133 (2018). Synthesis and evaluation of a novel bivalent selective antagonist for the mu-
1134 delta opioid receptor heterodimer that reduces morphine withdrawal in mice. J. Med.
1135 Chem. *61*, 6075-6086.
1136 21. Chefer, V.I., and Shippenberg, T.S. (2009). Augmentation of morphine-induced
1137 sensitization but reduction in morphine tolerance and reward in delta-opioid receptor
1138 knockout mice. Neuropsychopharmacology *34*, 887-898.
1139 22. Gomes, I., Fujita, W., Gupta, A., Saldanha, S.A., Negri, A., Pinello, C.E., Eberhart, C.,
1140 Roberts, E., Filizola, M., Hodder, P.*, et al.* (2013). Identification of a μ-δ opioid receptor
1141 heteromer-biased agonist with antinociceptive activity. Proc. Natl. Acad. Sci. U.S.A. *110*,
1142 12072-12077.
1143 23. Wang, D., Tawfik, V.L., Corder, G., Low, S.A., François, A., Basbaum, A.I., and Scherrer,
1144 G. (2018). Functional divergence of delta and mu opioid receptor organization in CNS
1145 pain circuits. Neuron *98*, 90-108.e105.
1146 24. Zhu, Y., King, M.A., Schuller, A.G., Nitsche, J.F., Reidl, M., Elde, R.P., Unterwald, E.,

1147 Pasternak, G.W., and Pintar, J.E. (1999). Retention of supraspinal delta-like analgesia
1148 and loss of morphine tolerance in delta opioid receptor knockout mice. Neuron *24*, 243-
1149 252.
1150 25. Egan, T.M., and North, R.A. (1981). Both mu and delta opiate receptors exist on the
1151 same neuron. Science *214*, 923-924.
1152 26. Wang, H.B., Zhao, B., Zhong, Y.Q., Li, K.C., Li, Z.Y., Wang, Q., Lu, Y.J., Zhang, Z.N., He,
1153 S.Q., Zheng, H.C., *et al*. (2010). Coexpression of δ- and μ-opioid receptors in nociceptive
1154 sensory neurons. Proc. Natl. Acad. Sci. U.S.A. *107*, 13117-13122.
1155 27. Chakrabarti, S., Liu, N.-J., and Gintzler, A.R. (2010). Formation of μ-/κ-opioid receptor
1156 heterodimer is sex-dependent and mediates female-specific opioid analgesia. Proc. Natl.
1157 Acad. Sci. U.S.A. *107*, 20115-20119.
1158 28. Jordan, B.A., and Devi, L.A. (1999). G-protein-coupled receptor heterodimerization
1159 modulates receptor function. Nature *399*, 697-700.
1160 29. Berg, K.A., Rowan, M.P., Gupta, A., Sanchez, T.A., Silva, M., Gomes, I., McGuire, B.A.,
1161 Portoghese, P.S., Hargreaves, K.M., Devi, L.A., and Clarke, W.P. (2012). Allosteric
1162 interactions between δ and κ opioid receptors in peripheral sensory neurons. Mol.
1163 Pharmacol. *81*, 264.
1164 30. Jacobs, B.A., Pando, M.M., Jennings, E.M., Jamshidi, R.J., Zamora, J.C., Chavera, T.S.,
1165 Clarke, W.P., and Berg, K.A. (2019). Signaling characteristics and functional regulation
1166 of delta opioid-kappa opioid receptor (DOP-KOP) heteromers in peripheral sensory
1167 neurons. Neuropharmacology *151*, 208-218.
1168 31. Jacobs, B.A., Pando, M.M., Jennings, E., Chavera, T.A., Clarke, W.P., and Berg, K.A.
1169 (2018). Allosterism within δ opioid-κ opioid receptor heteromers in peripheral sensory
1170 neurons: regulation of κ opioid agonist efficacy. Mol. Pharmacol. *93*, 376-386.
1171 32. Waldhoer, M., Fong, J., Jones, R.M., Lunzer, M.M., Sharma, S.K., Kostenis, E., Portoghese,
1172 P.S., and Whistler, J.L. (2005). A heterodimer-selective agonist shows in vivo relevance
1173 of G protein-coupled receptor dimers. Proc. Natl. Acad. Sci. U.S.A. *102*, 9050-9055.
1174 33. Gomes, I., Ayoub, M.A., Fujita, W., Jaeger, W.C., Pfleger, K.D.G., and Devi, L.A. (2016).
1175 G protein–coupled receptor heteromers. Annu. Rev. of Pharmacol. Toxicol. *56*, 403-425.
1176 34. Gurevich, V.V., and Gurevich, E.V. (2018). GPCRs and Signal Transducers: Interaction
1177 Stoichiometry. Trends Pharmacol. Sci. *39*, 672-684.
1178 35. Bellot, M., Galandrin, S., Boularan, C., Matthies, H.J., Despas, F., Denis, C., Javitch, J.,
1179 Mazères, S., Sanni, S.J., Pons, V., et al. (2015). Dual agonist occupancy of AT1-R-α2C-
1180 AR heterodimers results in atypical Gs-PKA signaling. Nat. Chem. Biol. *11*, 271-279.
1181 36. Ferré, S., Ciruela, F., Woods, A.S., Lluis, C., and Franco, R. (2007). Functional relevance
1182 of neurotransmitter receptor heteromers in the central nervous system. Trends Neurosci.
1183 *30*, 440-446.

1184 37. Ngamlertwong, N., Tsuchiya, H., Mochimaru, Y., Azuma, M., Kuchimaru, T., and
1185 Koshimizu, T.-a. (2021). Agonist dependency of the second phase access of β-arrestin
1186 2 to the heteromeric μ-V1b receptor. Sci. Rep. *11*, 15813.
1187 38. Jorand, R., Biswas, S., Wakefield, D.L., Tobin, S.J., Golfetto, O., Hilton, K., Ko, M., Ramos,
1188 J.W., Small, A.R., Chu, P., et al. (2016). Molecular signatures of mu opioid receptor and
1189 somatostatin receptor 2 in pancreatic cancer. Mol. Biol. Cell *27*, 3659-3672.
1190 39. Hübner, H., Schellhorn, T., Gienger, M., Schaab, C., Kaindl, J., Leeb, L., Clark, T., Möller,
1191 D., and Gmeiner, P. (2016). Structure-guided development of heterodimer-selective
1192 GPCR ligands. Nat. Commun. *7*, 12298.
1193 40. Callén, L., Moreno, E., Barroso-Chinea, P., Moreno-Delgado, D., Cortés, A., Mallol, J.,
1194 Casadó, V., Lanciego, J.L., Franco, R., Lluis, C., et al. (2012). Cannabinoid receptors CB1
1195 and CB2 form functional heteromers in brain. J. Biol. Chem. *287*, 20851-20865.
1196 41. Verma, V., Hasbi, A., O'Dowd, B.F., and George, S.R. (2010). Dopamine D1-D2 receptor
1197 Heteromer-mediated calcium release is desensitized by D1 receptor occupancy with or
1198 without signal activation: dual functional regulation by G protein-coupled receptor kinase
1199 2. J. Biol. Chem. *285*, 35092-35103.
1200 42. Filizola, M., Olmea, O., and Weinstein, H. (2002). Prediction of heterodimerization
1201 interfaces of G-protein coupled receptors with a new subtractive correlated mutation
1202 method. Protein Eng. Des. Sel. *15*, 881-885.
1203 43. Filizola, M., and Weinstein, H. (2002). Structural models for dimerization of G-protein
1204 coupled receptors: The opioid receptor homodimers. Pept. Sci. *66*, 317-325.
1205 44. Dijkman, P.M., Castell, O.K., Goddard, A.D., Munoz-Garcia, J.C., de Graaf, C., Wallace,
1206 M.I., and Watts, A. (2018). Dynamic tuneable G protein-coupled receptor monomer-
1207 dimer populations. Nat. Commun. *9*, 1710.
1208 45. Pan, Y.X. (2003). Expression of opioid receptors in mammalian cell lines. In Opioid
1209 Research: Methods and Protocols, Z.Z. Pan, ed. (Totowa, NJ: Humana Press), pp. 17-28.
1210 46. Liu, X., Kai, M., Jin, L., and Wang, R. (2009). Computational study of the
1211 heterodimerization between μ and δ receptors. Journal of Computer-Aided Molecular
1212 Design *23*, 321-332.
1213 47. Marino, K.A., Prada-Gracia, D., Provasi, D., and Filizola, M. (2016). Impact of lipid
1214 composition and receptor conformation on the spatio-temporal organization of μ-opioid
1215 receptors in a multi-component plasma membrane model. PLoS Comput. Biol. *12*,
1216 e1005240.
1217 48. Meral, D., Provasi, D., Prada-Gracia, D., Möller, J., Marino, K., Lohse, M.J., and Filizola, M.
1218 (2018). Molecular details of dimerization kinetics reveal negligible populations of
1219 transient μ-opioid receptor homodimers at physiological concentrations. Sci. Rep. *8*,
1220 7705.

1221 49. Grasberger, B., Minton, A.P., DeLisi, C., and Metzger, H. (1986). Interaction between
1222 proteins localized in membranes. Proc. Natl. Acad. Sci. U.S.A. *83*, 6258-6262.
1223 50. Yekkirala, A.S., Kalyuzhny, A.E., and Portoghese, P.S. (2010). Standard opioid agonists
1224 activate heteromeric opioid receptors: evidence for morphine and [d-Ala(2)-MePhe(4)-
1225 Glyol(5)]enkephalin as selective μ-δ agonists. ACS Chem. Neurosci. *1*, 146-154.
1226 51. Fagan, R.R., Lee, D.F., Geron, M., Scherrer, G., von Zastrow, M., and Ehrlich, A.T. (2024).
1227 Selective targeting of mu opioid receptors to primary cilia. Cell Rep. *43*. 10.
1228 52. Décaillot, F.M., Rozenfeld, R., Gupta, A., and Devi, L.A. (2008). Cell surface targeting of
1229 mu-delta opioid receptor heterodimers by RTP4. Proc. Natl. Acad. Sci. U.S.A. *105*, 16045-
1230 16050.
1231 53. Bao, F., Li, C.L., Chen, X.Q., Lu, Y.J., Bao, L., and Zhang, X. (2018). Clinical opioids
1232 differentially induce co-internalization of μ- and δ-opioid receptors. Mol. Pain *14*,
1233 1744806918769492.
1234 54. Rozenfeld, R., and Devi, L.A. (2007). Receptor heterodimerization leads to a switch in
1235 signaling: β-arrestin2-mediated ERK activation by μ-δ opioid receptor heterodimers.
1236 FASEB J. *21*, 2455-2465.
1237 55. Grimes, J., Lanoiselée, Y., Miljus, T., O'Brien, S.L., Stepniewski, T.M., Medel-Lacruz, B.,
1238 Baidya, M., Makarova, M., Mistry, R., *et al.* (2023). Plasma membrane preassociation
1239 drives β-arrestin coupling to receptors and activation. Cell *186*, 2238-2255. E20.
1240 56. Suzuki, K.G.N., Fujiwara, T.K., Edidin, M., and Kusumi, A. (2007). Dynamic recruitment
1241 of phospholipase Cγ at transiently immobilized GPI-anchored receptor clusters induces
1242 IP_3–Ca^{2+} signaling: single-molecule tracking study 2. J. Cell Biol. *177*, 731-742.
1243 57. Suzuki, K.G.N., Fujiwara, T.K., Sanematsu, F., Iino, R., Edidin, M., and Kusumi, A. (2007).
1244 GPI-anchored receptor clusters transiently recruit Lyn and Gα for temporary cluster
1245 immobilization and Lyn activation: single-molecule tracking study 1. J. Cell Biol. *177*,
1246 717-730.
1247 58. Kusumi, A., Tsunoyama, T.A., Suzuki, K.G.N., Fujiwara, T.K., and Aladag, A. (2024)
1248 Transient, nano-scale, liquid-like molecular assemblies coming of age. Curr. Opinion Cell
1249 Biol. *89,* 102394.
1250 59. Metcalf, M.D., Yekkirala, A.S., Powers, M.D., Kitto, K.F., Fairbanks, C.A., Wilcox, G.L.,
1251 and Portoghese, P.S. (2012). The δ opioid receptor agonist SNC80 selectively activates
1252 heteromeric μ-δ opioid receptors. ACS Chem. Neurosci. *3*, 505-509.
1253 60. Asher, W.B., Geggier, P., Holsey, M.D., Gilmore, G.T., Pati, A.K., Meszaros, J., Terry, D.S.,
1254 Mathiasen, S., Kaliszewski, M.J., McCauley, M.D.*, et al.* (2021). Single-molecule FRET
1255 imaging of GPCR dimers in living cells. Nat. Methods *18*, 397-405.
1256 61. Cechova, K., Lan, C., Macik, M., Barthes, N.P.F., Jung, M., and Ulbrich, M.H. (2021). Kappa
1257 but not delta or mu opioid receptors form homodimers at low membrane densities. Cell.

1258 Mol. Life Sci. *78*, 7557-7568.
1259 62. Drakopoulos, A., Koszegi, Z., Lanoiselée, Y., Hübner, H., Gmeiner, P., Calebiro, D., and
1260 Decker, M. (2020). Investigation of inactive-state κ opioid receptor homodimerization via
1261 single-molecule microscopy using new antagonistic fluorescent probes. J. Med. Chem.
1262 *63*, 3596-3609.
1263 63. Baiula, M. (2021). Monitoring Opioid Receptor Interaction in Living Cells by
1264 Bioluminescence Resonance Energy Transfer (BRET). Methods Mol. Biol. *2201*, 35-43.
1265 64. Cvejic, S., and Devi, L.A. (1997). Dimerization of the delta opioid receptor: implication
1266 for a role in receptor internalization. J. Biol. Chem. *272*, 26959-26964.
1267 65. Gomes, I., Filipovska, J., Jordan, B.A., and Devi, L.A. (2002). Oligomerization of opioid
1268 receptors. Methods *27*, 358-365.
1269 66. He, L., Fong, J., von Zastrow, M., and Whistler, J.L. (2002). Regulation of opioid receptor
1270 trafficking and morphine tolerance by receptor oligomerization. Cell *108*, 271-282.
1271 67. Johnston, J.M., Aburi, M., Provasi, D., Bortolato, A., Urizar, E., Lambert, N.A., Javitch, J.A.,
1272 and Filizola, M. (2011). Making structural sense of dimerization interfaces of delta opioid
1273 receptor homodimers. Biochemistry *50*, 1682-1690.
1274 68. Manglik, A., Kruse, A.C., Kobilka, T.S., Thian, F.S., Mathiesen, J.M., Sunahara, R.K., Pardo,
1275 L., Weis, W.I., Kobilka, B.K., and Granier, S. (2012). Crystal structure of the μ-opioid
1276 receptor bound to a morphinan antagonist. Nature *485*, 321-326.
1277 69. Kaneko, S., Imai, S., Uchikubo-Kamo, T., Hisano, T., Asao, N., Shirouzu, M., and
1278 Shimada, I. (2024). Structural and dynamic insights into the activation of the μ-opioid
1279 receptor by an allosteric modulator. Nat. Commun. *15*, 3544.
1280 70. Mahoney, J.P., and Sunahara, R.K. (2016). Mechanistic insights into GPCR–G protein
1281 interactions. Curr. Opin. Struct. Biol. *41*, 247-254.
1282 71. Whorton, M.R., Bokoch, M.P., Rasmussen, S.G.F., Huang, B., Zare, R.N., Kobilka, B., and
1283 Sunahara, R.K. (2007). A monomeric G protein-coupled receptor isolated in a high-
1284 density lipoprotein particle efficiently activates its G protein. Proc. Natl. Acad. Sci. U.S.A.
1285 *104*, 7682-7687.
1286 72. Nitsche, J.F., Schuller, A.G., King, M.A., Zengh, M., Pasternak, G.W., and Pintar, J.E.
1287 (2002). Genetic dissociation of opiate tolerance and physical dependence in delta-opioid
1288 receptor-1 and preproenkephalin knock-out mice. J. Neurosci. *22*, 10906-10913.
1289 73. Xie, W.Y., He, Y., Yang, Y.R., Li, Y.F., Kang, K., Xing, B.M., and Wang, Y. (2009).
1290 Disruption of cdk5-associated phosphorylation of residue threonine-161 of the δ-opioid
1291 receptor: impaired receptor function and attenuated morphine antinociceptive tolerance.
1292 J. Neurosci. *29*, 3551.

1293 74. Gaborit, M., and Massotte, D. (2023). Therapeutic potential of opioid receptor
1294 heteromers in chronic pain and associated comorbidities. Br. J. Pharmacol. *180*, 994-
1295 1013.
1296 75. Rogacki, M.K., Golfetto, O., Tobin, S.J., Li, T., Biswas, S., Jorand, R., Zhang, H., Radoi,
1297 V., Ming, Y., Svenningsson, P., et al. (2018). Dynamic lateral organization of opioid
1298 receptors (kappa, mu_{wt} and mu_{N40D}) in the plasma membrane at the nanoscale level.
1299 Traffic *19*, 690-709.
1300 76. Kwon, Y., Mehta, S., Clark, M., Walters, G., Zhong, Y., Lee, H.N., Sunahara, R.K., and
1301 Zhang, J. (2022). Non-canonical β-adrenergic activation of ERK at endosomes. Nature
1302 *611*, 173-179.
1303 77. Nguyen, A.H., Thomsen, A.R.B., Cahill, T.J., 3rd, Huang, R., Huang, L.Y., Marcink, T.,
1304 Clarke, O.B., Heissel, S., Masoudi, A., Ben-Hail, D., et al. (2019). Structure of an
1305 endosomal signaling GPCR-G protein-β-arrestin megacomplex. Nat. Struct. Mol. Biol. *26*,
1306 1123-1131.
1307 78. Kasai, R.S., Suzuki, K.G.N., Prossnitz, E.R., Koyama-Honda, I., Nakada, C., Fujiwara, T.K.,
1308 and Kusumi, A. (2011). Full characterization of GPCR monomer-dimer dynamic
1309 equilibrium by single molecule imaging. J. Cell Biol. *192*, 463-480.
1310 79. Nakamura, A., Oki, C., Kato, K., Fujinuma, S., Maryu, G., Kuwata, K., Yoshii, T., Matsuda,
1311 M., Aoki, K., and Tsukiji, S. (2020). Engineering Orthogonal, Plasma Membrane-Specific
1312 SLIPT Systems for Multiplexed Chemical Control of Signaling Pathways in Living Single
1313 Cells. ACS Chem. Biol. *15*, 1004-1015.
1314 80. Shaner, N.C., Campbell, R.E., Steinbach, P.A., Giepmans, B.N.G., Palmer, A.E., and Tsien,
1315 R.Y. (2004). Improved monomeric red, orange and yellow fluorescent proteins derived
1316 from *Discosoma* sp. red fluorescent protein. Nat. Biotechnol. *22*, 1567-1572.
1317 81. Lindberg, F.P., Gresham, H.D., Schwarz, E., and Brown, E.J. (1993). Molecular cloning
1318 of integrin-associated protein: an immunoglobulin family member with multiple
1319 membrane-spanning domains implicated in alpha v beta 3-dependent ligand binding. J.
1320 Cell Biol. *123*, 485-496.
1321 82. James, J.R., Oliveira, M.I., Carmo, A.M., Iaboni, A., and Davis, S.J. (2006). A rigorous
1322 experimental framework for detecting protein oligomerization using bioluminescence
1323 resonance energy transfer. Nat. Methods *3*, 1001-1006.
1324 83. Fukuda, K., Kato, S., Mori, K., Nishi, M., and Takeshima, H. (1993). Primary structures
1325 and expression from cDNAs of rat opioid receptor δ-and μ-subtypes. FEBS Lett. *327*,
1326 311-314.
1327 84. Schulz, R., Wehmeyer, A., and Schulz, K. (2002). Opioid receptor types selectively
1328 cointernalize with G protein-coupled receptor kinases 2 and 3. J. Pharmacol. Exp. Ther.
1329 *300*, 376.

85. Schindelin, J., Arganda-Carreras, I., Frise, E., Kaynig, V., Longair, M., Pietzsch, T., Preibisch, S., Rueden, C., Saalfeld, S., Schmid, B., et al. (2012). Fiji: an open-source platform for biological-image analysis. Nat. Methods *9*, 676-682.
86. Fujiwara, T.K., Takeuchi, S., Kalay, Z., Nagai, Y., Tsunoyama, T.A., Kalkbrenner, T., Iwasawa, K., Ritchie, K.P., Suzuki, K.G.N., and Kusumi, A. (2023). Development of ultrafast camera-based single fluorescent-molecule imaging for cell biology. J. Cell Biol. *222*, e202110160.
87. Tsunoyama, T.A., Watanabe, Y., Goto, J., Naito, K., Kasai, R.S., Suzuki, K.G.N., Fujiwara, T.K., and Kusumi, A. (2018). Super-long single-molecule tracking reveals dynamic-anchorage-induced integrin function. Nat. Chem. Biol. *14*, 497-506.
88. Koyama-Honda, I., Ritchie, K., Fujiwara, T., Iino, R., Murakoshi, H., Kasai, R.S., and Kusumi, A. (2005). Fluorescence imaging for monitoring the colocalization of two single molecules in living cells. Biophys. J. *88*, 2126-2136.
89. Murakoshi, H., Iino, R., Kobayashi, T., Fujiwara, T., Ohshima, C., Yoshimura, A., and Kusumi, A. (2004). Single-molecule imaging analysis of Ras activation in living cells. Proc. Natl. Acad. Sci. U.S.A. *101*, 7317-7322.
90. Fujiwara, T.K., Iwasawa, K., Kalay, Z., Tsunoyama, T.A., Watanabe, Y., Umemura, Y.M., Murakoshi, H., Suzuki, K.G.N., Nemoto, Y.L., Morone, N.*, et al.* (2016). Confined diffusion of transmembrane proteins and lipids induced by the same actin meshwork lining the plasma membrane. Mol. Biol. Cell *27*, 1101-1119.
91. Hagg, T. (2007). Intracerebral Infusion of Neurotrophic Factors. In Neuroprotection Methods and Protocols, T. Borsello, ed. (Humana Press), pp. 167-180.

Figure 1

A DM heterodimerization: images and trajectories

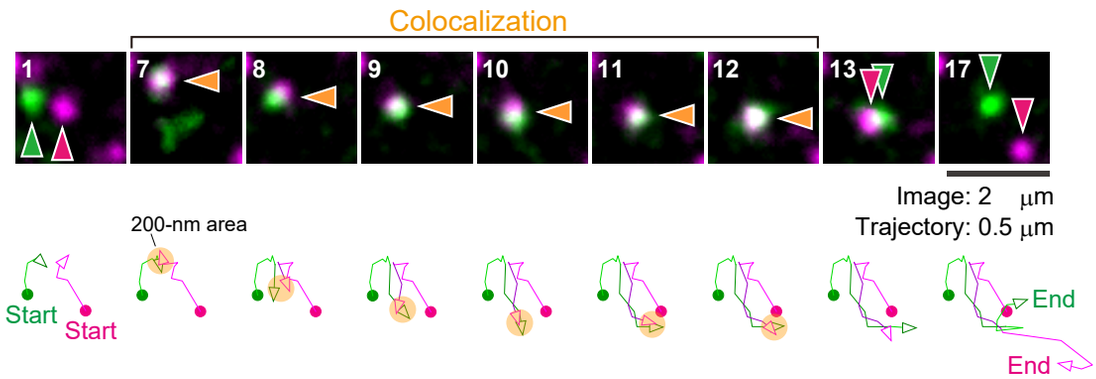

B-D Hetero-colocalization indexes and heterodimer lifetimes (dissociation rate constants)

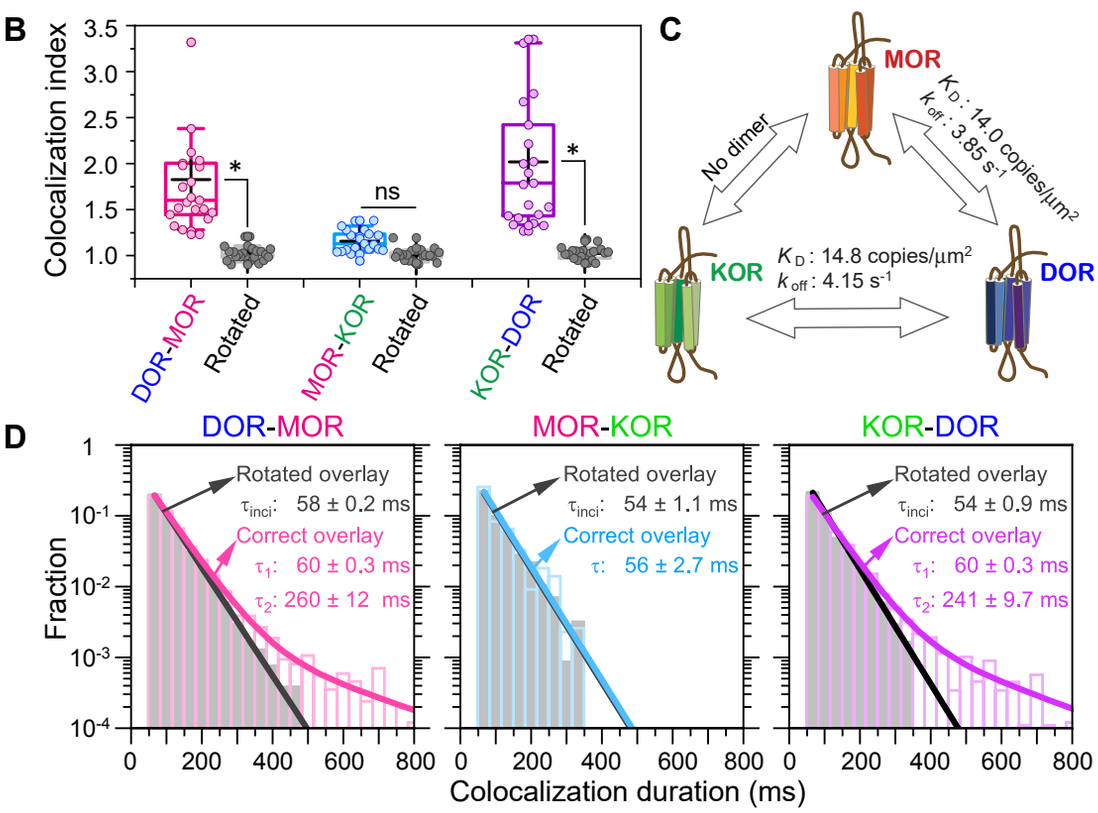

E Homology of rat OR amino acid sequences

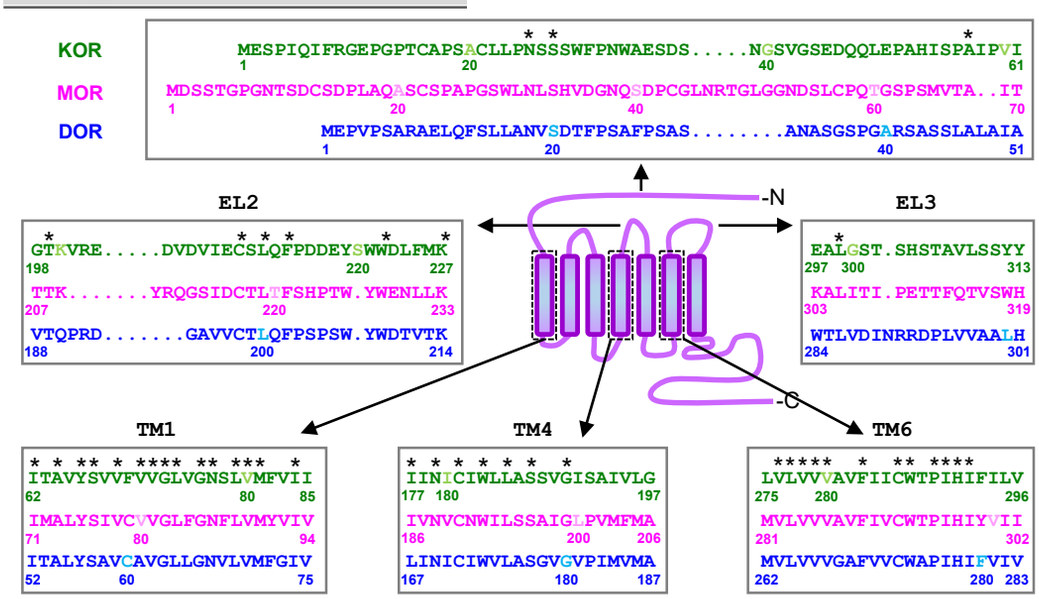

Figure 2

A N- and C-terminal deletions do not affect DK heterodimerization

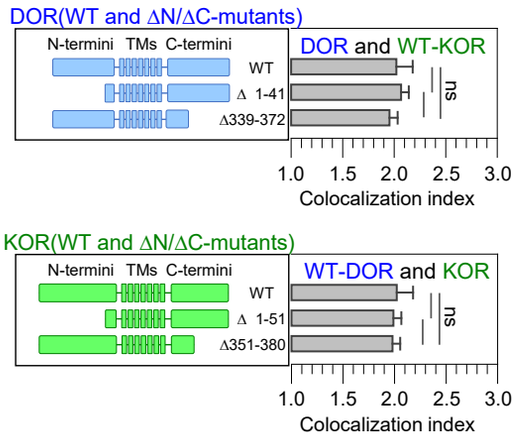

B

Domains	amino-acid numbers
NTerm^{KOR}	KOR(1-61)
NTerm^{MOR}	MOR(1-70)
NTerm^{DOR}	DOR(1-51)
EL2^{MOR}	MOR(207-233)
EL2^{DOR}	DOR(188-214)
EL3^{KOR}	KOR(297-312)
EL3^{MOR}	MOR(303-319)
EL3^{DOR}	DOR(284-301)
TM1^{KOR}	KOR(62-85)
TM1^{MOR}	MOR(71-94)
TM1^{DOR}	DOR(52-75)
TM4^{KOR}	KOR(177-197)
TM4^{MOR}	MOR(186-206)
TM4^{DOR}	DOR(167-187)
TM6^{KOR}	KOR(275-296)
Peptides	
TM1^{MOR}	MOR(71-99)
Nterm-TM1^{MOR}	MOR(53-99)
TM1^{DOR}	DOR(52-80)
TM^{LDLR}-TM4^{DOR}	LDLR(785-822)-SGSGx3-DOR(167-187)

C MOR (w/DOR-seq) vs. WT-KOR (left) and DOR (w/MOR-seq) vs. WT-KOR (right)

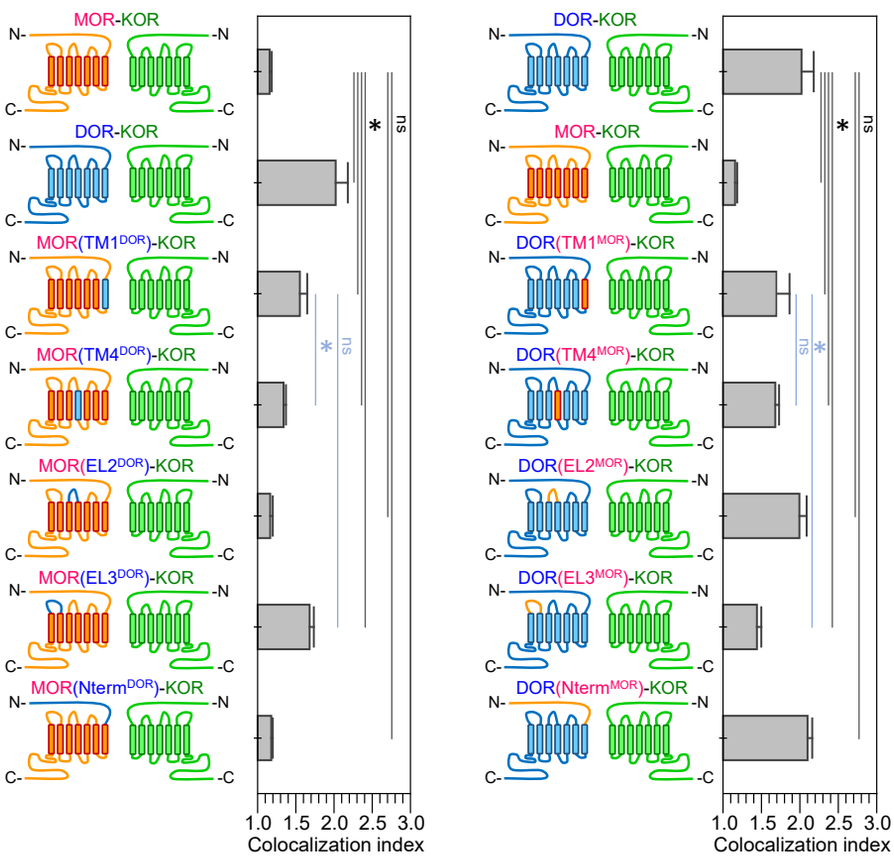

D + Soluble EL3 domain peptides

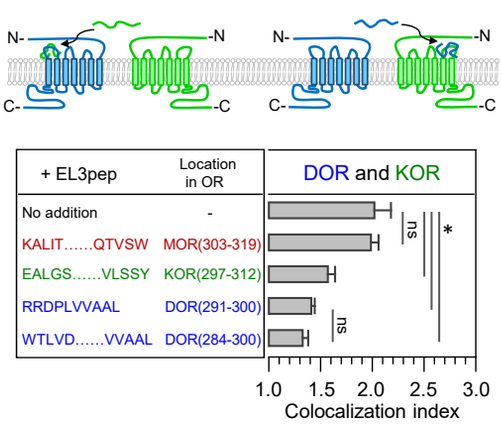

E DOR's TM1 and TM4 bind to KOR

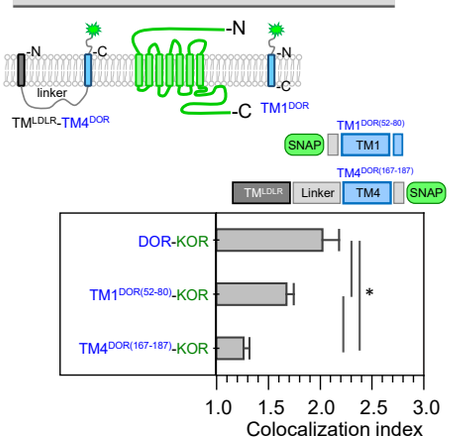

Figure 3

A DOR's aa22-42 and MOR's aa32-61 in the extracellular N-terminal domains: DM heterodimerization

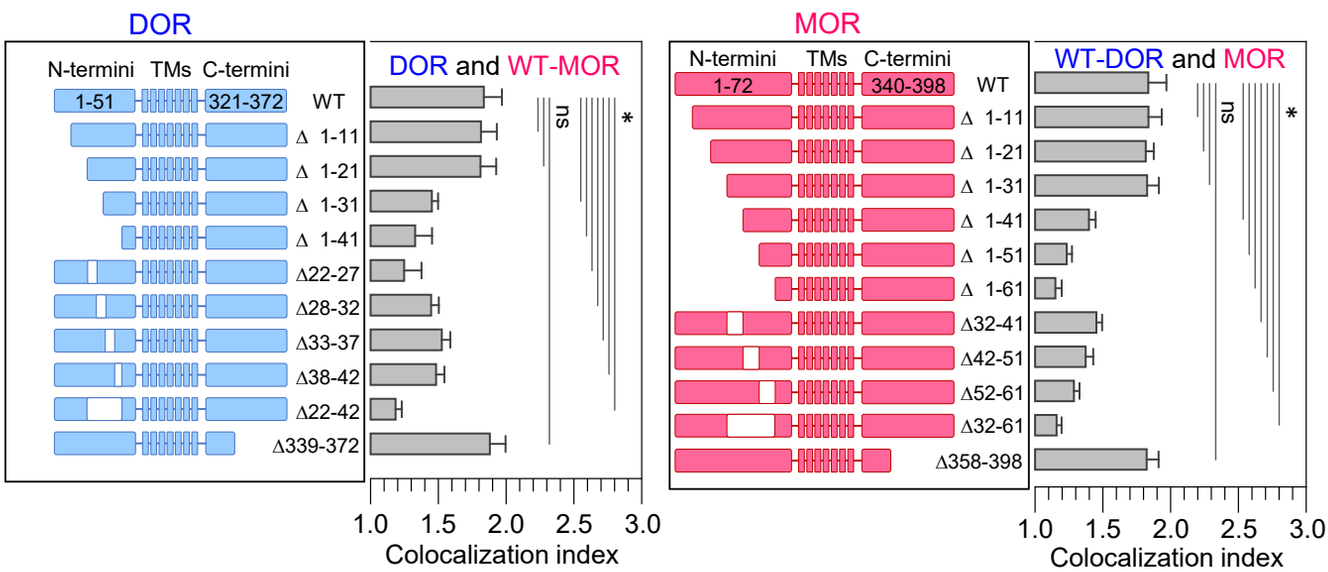

B Heterodimer durations for DOR(Δ22-42)-MOR (left) and DOR-MOR(Δ32-61) (right)

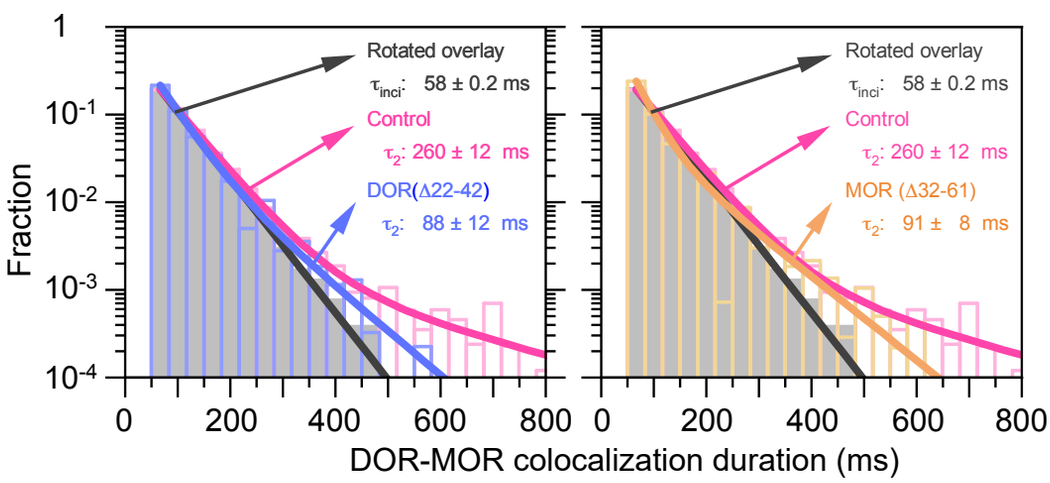

C DOR (w/KOR-seq) vs. WT-MOR (left) and MOR (w/KOR-seq) vs. WT-DOR (right)

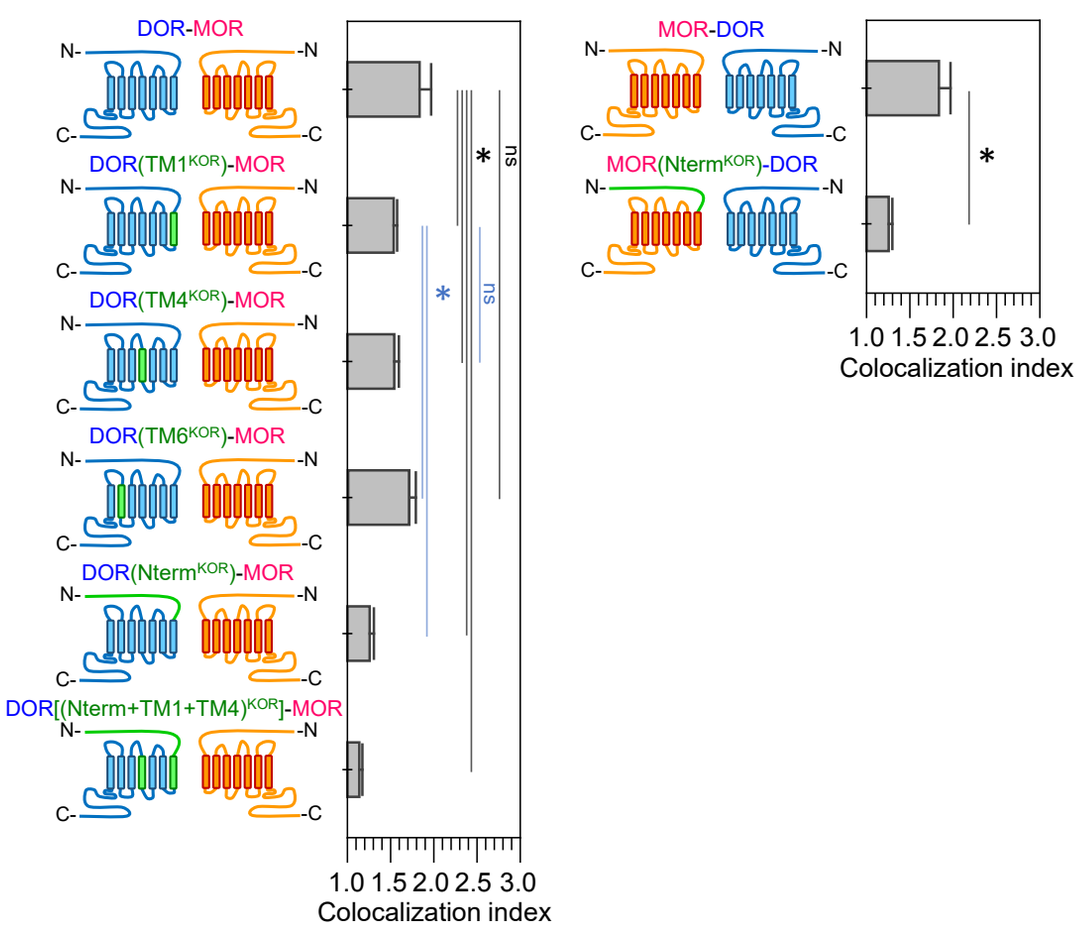

Figure 4

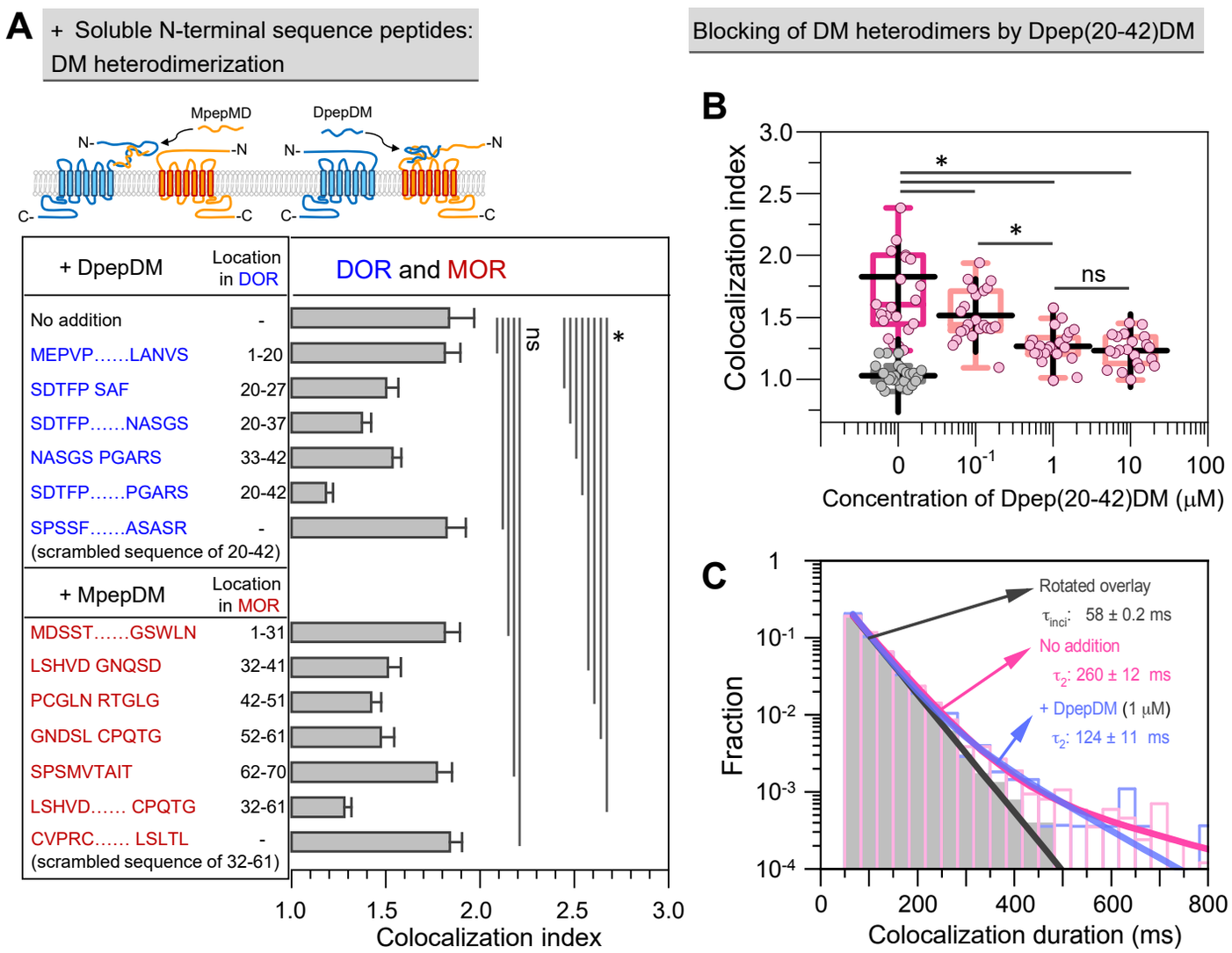
A
+ Soluble N-terminal sequence peptides: DM heterodimerization
MpepMD
DpepDM
N-
-N
C-
-C
+ DpepDM
Location in DOR
DOR and MOR
No addition
MEPVP……LANVS
SDTFP SAF
SDTFP……NASGS
NASGS PGARS
SDTFP……PGARS
SPSSF……ASASR
(scrambled sequence of 20-42)
+ MpepDM
Location in MOR
MDSST……GSWLN
LSHVD GNQSD
PCGLN RTGLG
GNDSL CPQTG
SPSMVTAIT
LSHVD…… CPQTG
CVPRC…… LSLTL
(scrambled sequence of 32-61)
ns
*
Colocalization index
Blocking of DM heterodimers by Dpep(20-42)DM
B
Colocalization index
Concentration of Dpep(20-42)DM (μM)
C
Fraction
Rotated overlay
τinci: 58 ± 0.2 ms
No addition
τ2: 260 ± 12 ms
+ DpepDM (1 μM)
τ2: 124 ± 11 ms
Colocalization duration (ms)

Figure 5

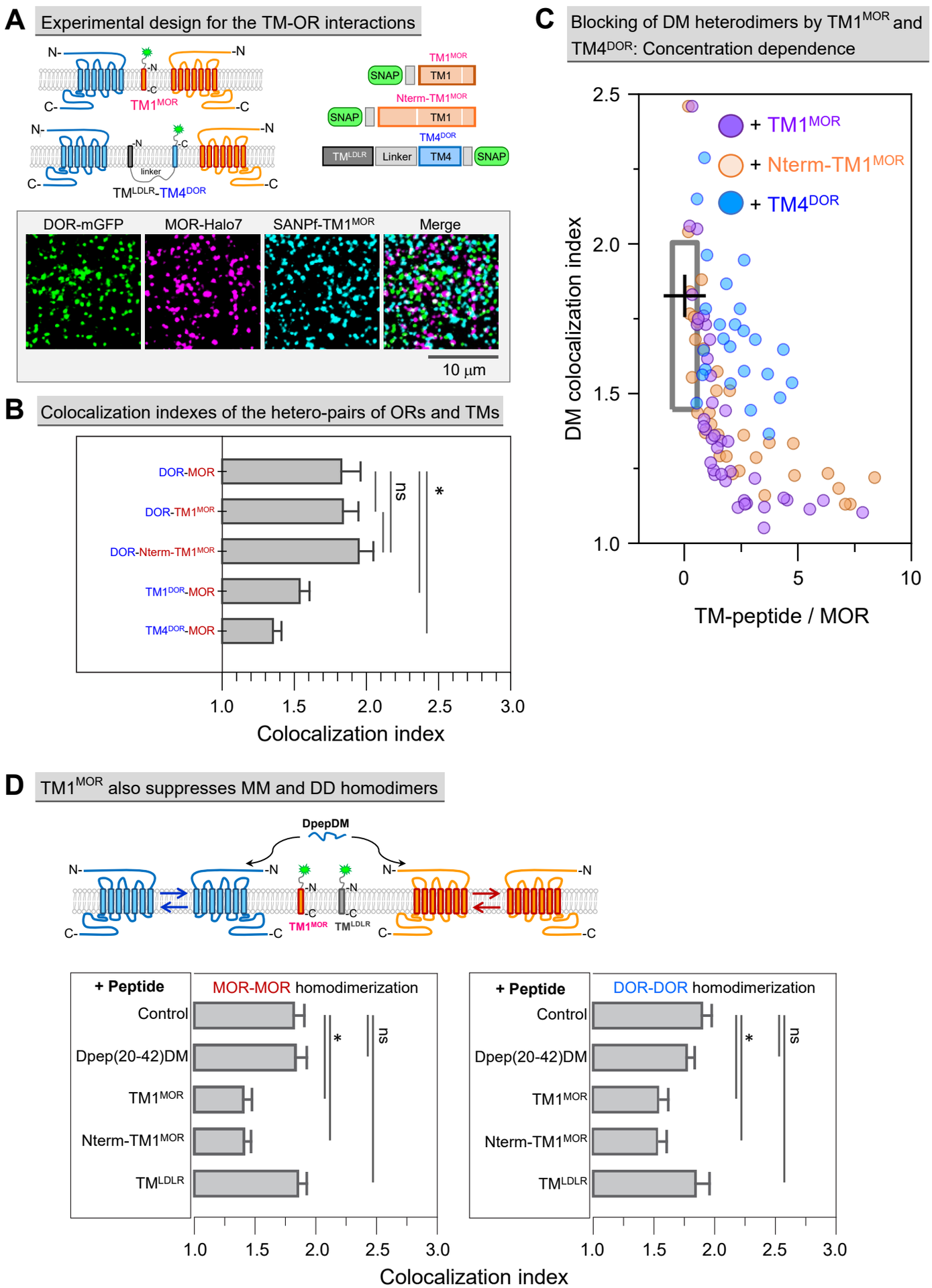
A
Experimental design for the TM-OR interactions
N-
-N
-C
C-
TM1MOR
TMLDLR-TM4DOR
linker
SNAP
TM1MOR
TM1
Nterm-TM1MOR
TM4DOR
TMLDLR
Linker
TM4
DOR-mGFP
MOR-Halo7
SANPf-TM1MOR
Merge
10 µm
B
Colocalization indexes of the hetero-pairs of ORs and TMs
DOR-MOR
DOR-TM1MOR
DOR-Nterm-TM1MOR
TM1DOR-MOR
TM4DOR-MOR
ns
*
1.0
1.5
2.0
2.5
3.0
Colocalization index
C
Blocking of DM heterodimers by TM1MOR and TM4DOR: Concentration dependence
+ TM1MOR
+ Nterm-TM1MOR
+ TM4DOR
DM colocalization index
TM-peptide / MOR
0
5
10
D
TM1MOR also suppresses MM and DD homodimers
DpepDM
TM1MOR
TMLDLR
+ Peptide
MOR-MOR homodimerization
DOR-DOR homodimerization
Control
Dpep(20-42)DM
TM1MOR
Nterm-TM1MOR
TMLDLR
Colocalization index

Figure 6

A PCCF of DOR-MOR

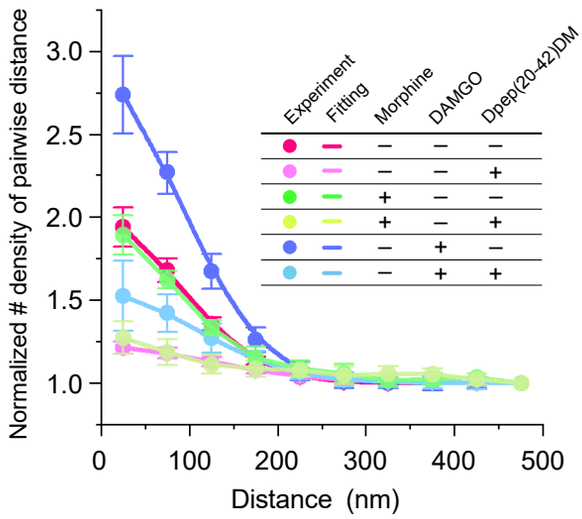

B Dpep(20-42)DM suppresses DM heterodimers both before and after the M-agonist addition

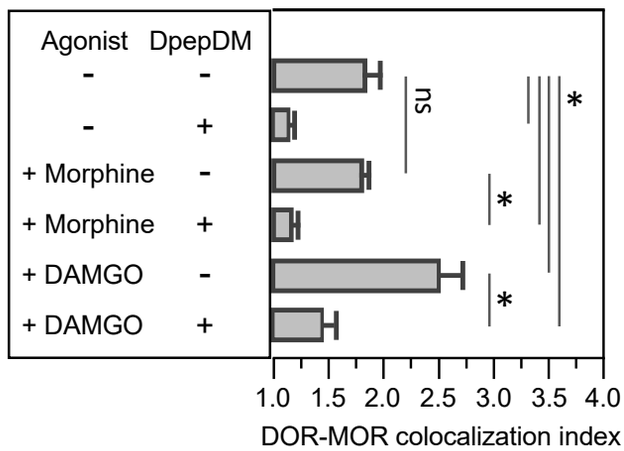

C DM heterodimer lifetimes

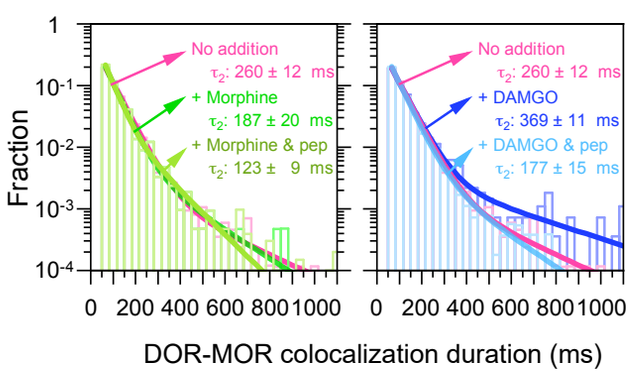

D DAMGO ± Dpep(20-42)DM effect on DM heterodimers

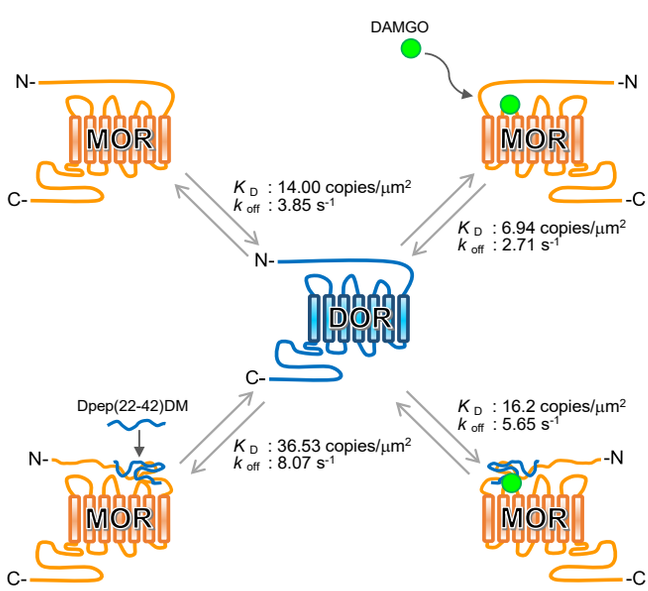

E Summary of K_D, k_{off}, and, k_{on} for homo- and heterodimers

		K_D (copies/μm^2)	k_{off} (/s)	k_{on} (μm^2/copies/s)
KK homodimer		5.87	6.71	1.14
DD homodimer		16.42	8.00	0.49
+ Morphine		18.08	8.13	0.45
MM homodimer		15.24	8.47	0.56
+ Morphine		19.69	8.48	0.43
+ DAMGO		8.34	5.35	0.64
DM heterodimer				
No addition		14.00	3.85	0.28
	+DpepDM	36.53	8.07	0.22
+ Morphine		15.36	5.35	0.35
	+DpepDM	23.65	8.13	0.34
+ DAMGO		6.94	2.71	0.39
	+DpepDM	16.20	5.65	0.35
DK heterodimer				
No addition		14.76	4.15	0.28
	+DpepEL3	29.30	6.10	0.21

Figure 7

A Effect of DM heterodimer blocker Dpep(20-42)DM on agonist-induced MOR signaling and trafficking

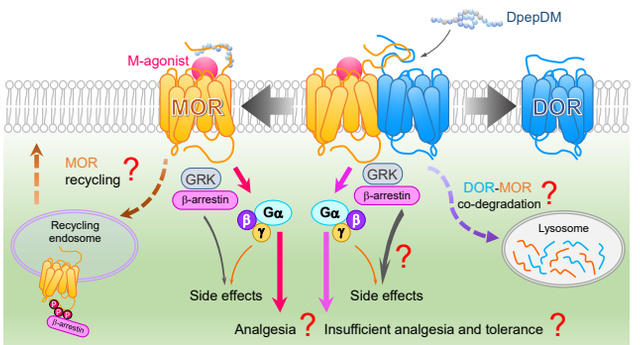

B DpepDM suppresses the DM co-internalization induced by DAMGO

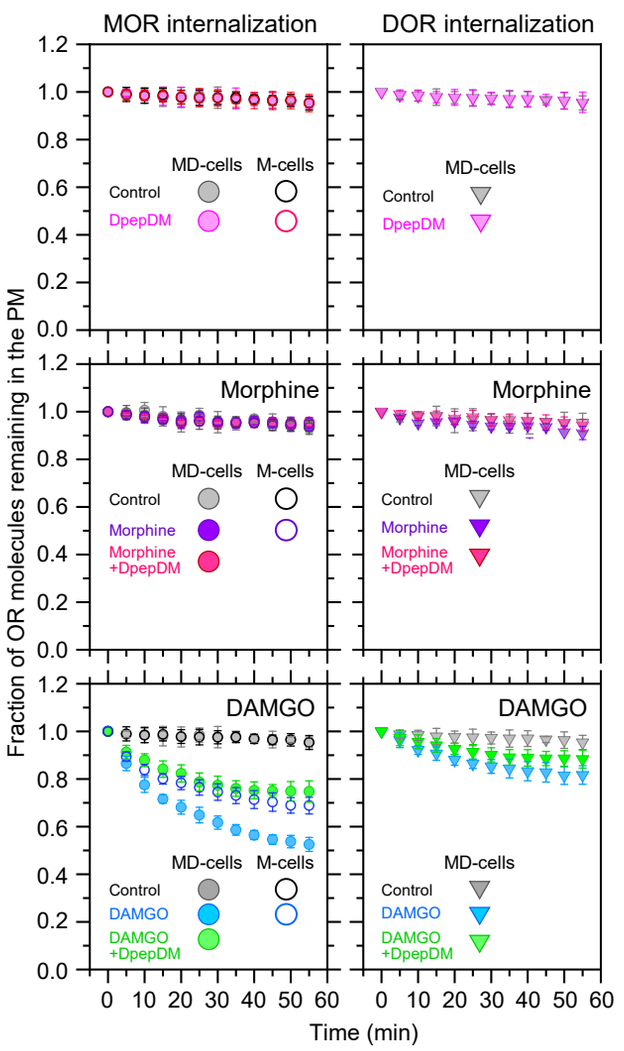

C Affinity of a single molecule of M*DAMGO to internalization machinery

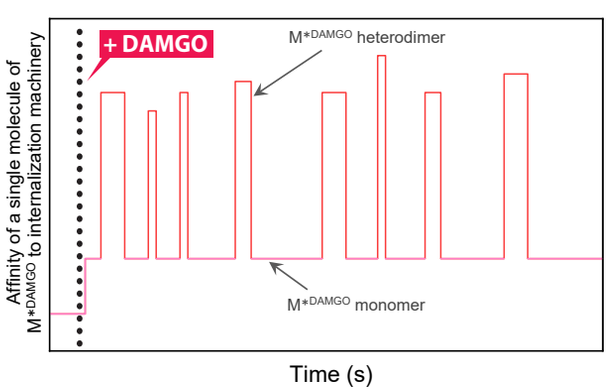

D Dpep(20-42)DM lowers the DOR-enhanced MOR signals after the M-agonist addition

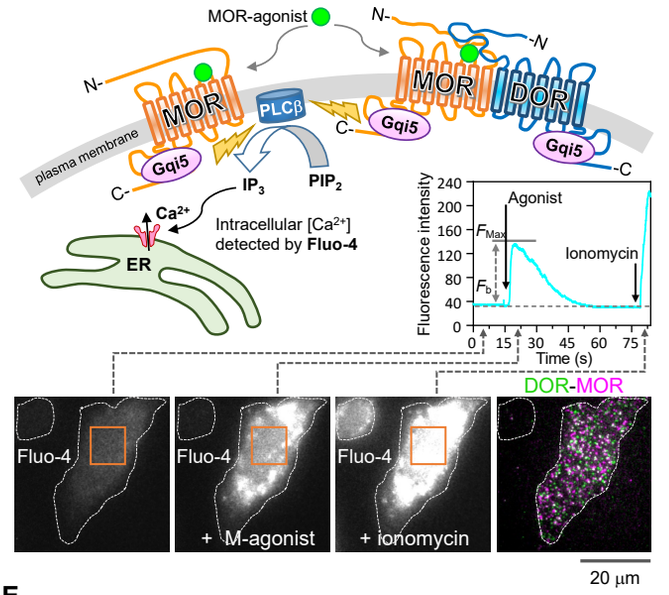

E

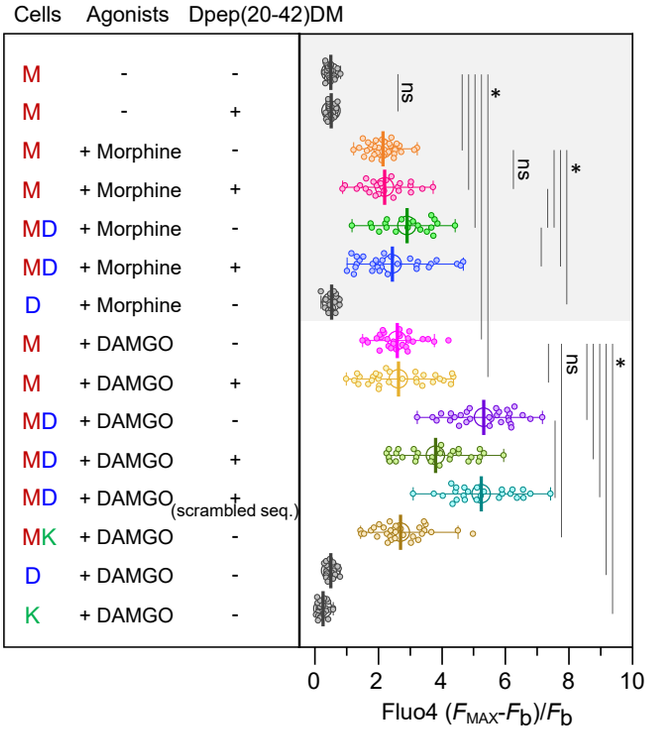

F Dpep(20-42)DM suppresses the development of morphine tolerance

G

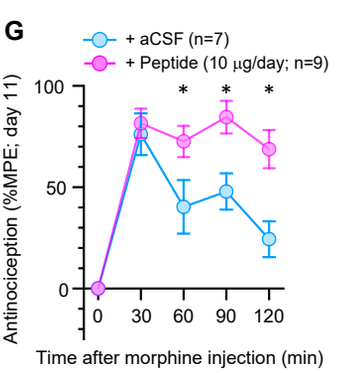

H

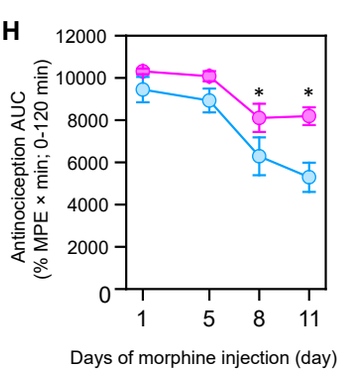

Figure S1

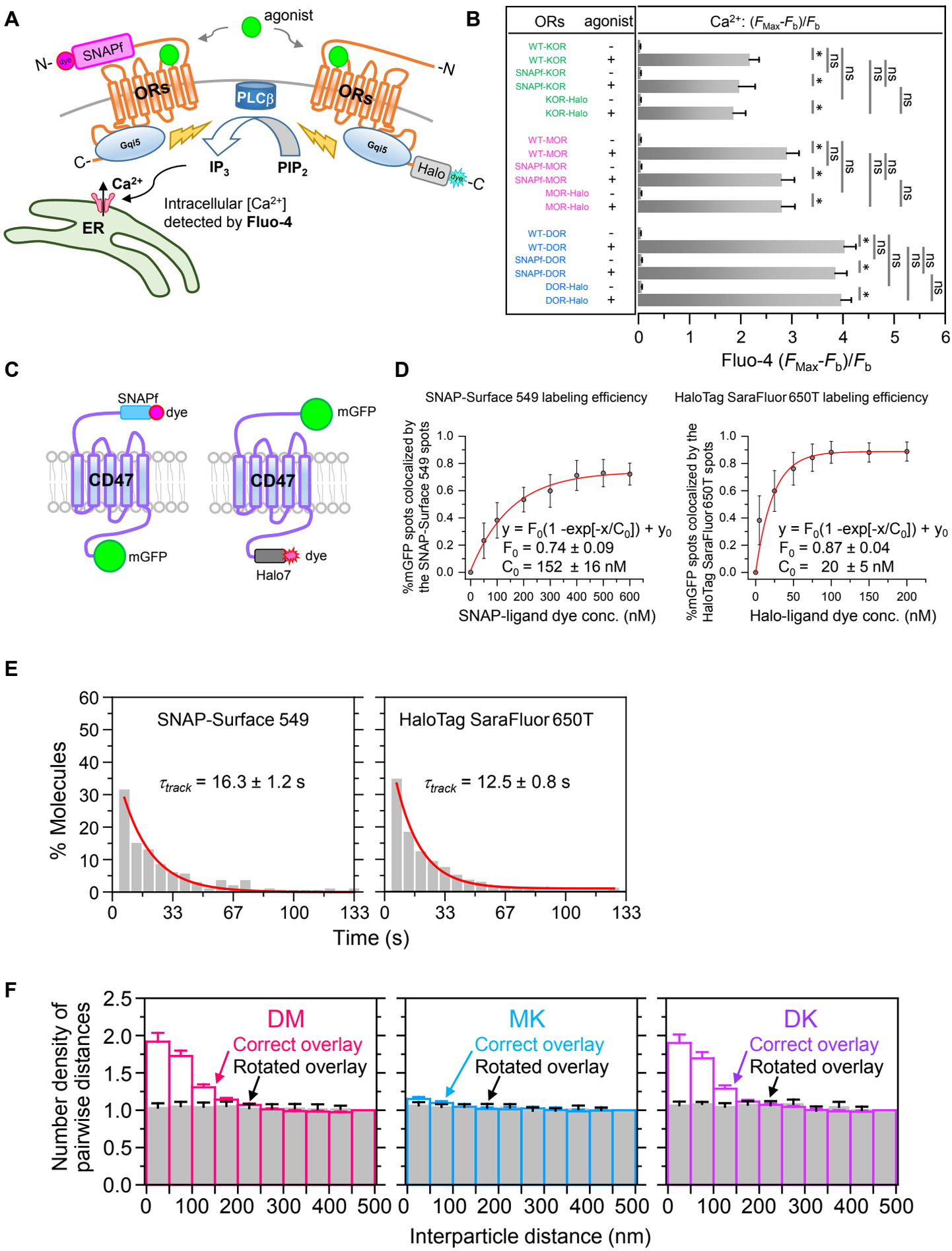
A
agonist
N-
SNAPf
dye
ORs
PLCβ
ORs
-N
Gqi5
Gqi5
C-
IP3
PIP2
Halo
dye
-C
Ca2+
ER
Intracellular [Ca2+]
detected by Fluo-4
B
ORs
agonist
Ca2+: (FMax-Fb)/Fb
WT-KOR
WT-KOR
SNAPf-KOR
SNAPf-KOR
KOR-Halo
KOR-Halo
WT-MOR
WT-MOR
SNAPf-MOR
SNAPf-MOR
MOR-Halo
MOR-Halo
WT-DOR
WT-DOR
SNAPf-DOR
SNAPf-DOR
DOR-Halo
DOR-Halo
Fluo-4 (FMax-Fb)/Fb
C
SNAPf
dye
CD47
mGFP
mGFP
CD47
dye
Halo7
D
SNAP-Surface 549 labeling efficiency
%mGFP spots colocalized by the SNAP-Surface 549 spots
y = F0(1 -exp[-x/C0]) + y0
F0 = 0.74 ± 0.09
C0 = 152 ± 16 nM
SNAP-ligand dye conc. (nM)
HaloTag SaraFluor 650T labeling efficiency
%mGFP spots colocalized by the HaloTag SaraFluor 650T spots
y = F0(1 -exp[-x/C0]) + y0
F0 = 0.87 ± 0.04
C0 = 20 ± 5 nM
Halo-ligand dye conc. (nM)
E
SNAP-Surface 549
τtrack = 16.3 ± 1.2 s
HaloTag SaraFluor 650T
τtrack = 12.5 ± 0.8 s
% Molecules
Time (s)
F
DM
Correct overlay
Rotated overlay
MK
Correct overlay
Rotated overlay
DK
Correct overlay
Rotated overlay
Number density of pairwise distances
Interparticle distance (nm)

Figure S2

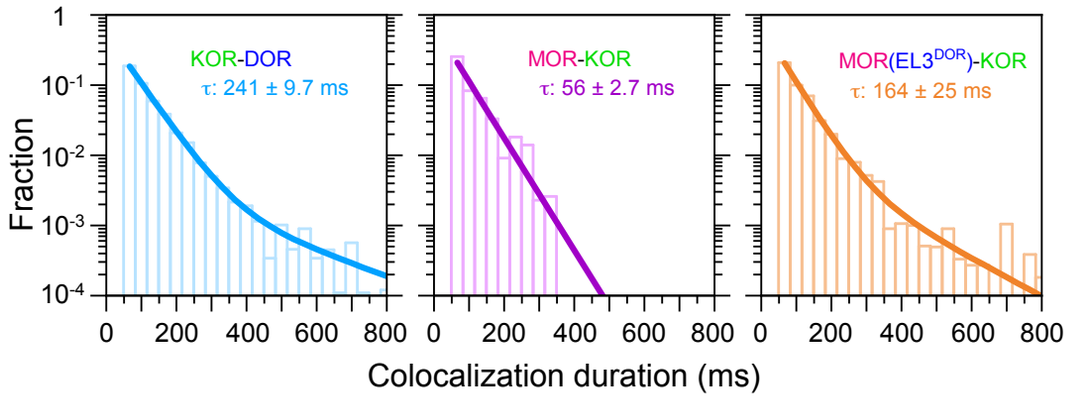
KOR-DOR
τ: 241 ± 9.7 ms
MOR-KOR
τ: 56 ± 2.7 ms
MOR(EL3DOR)-KOR
τ: 164 ± 25 ms
Fraction
1
10-1
10-2
10-3
10-4
0
200
400
600
800
Colocalization duration (ms)

Figure S3

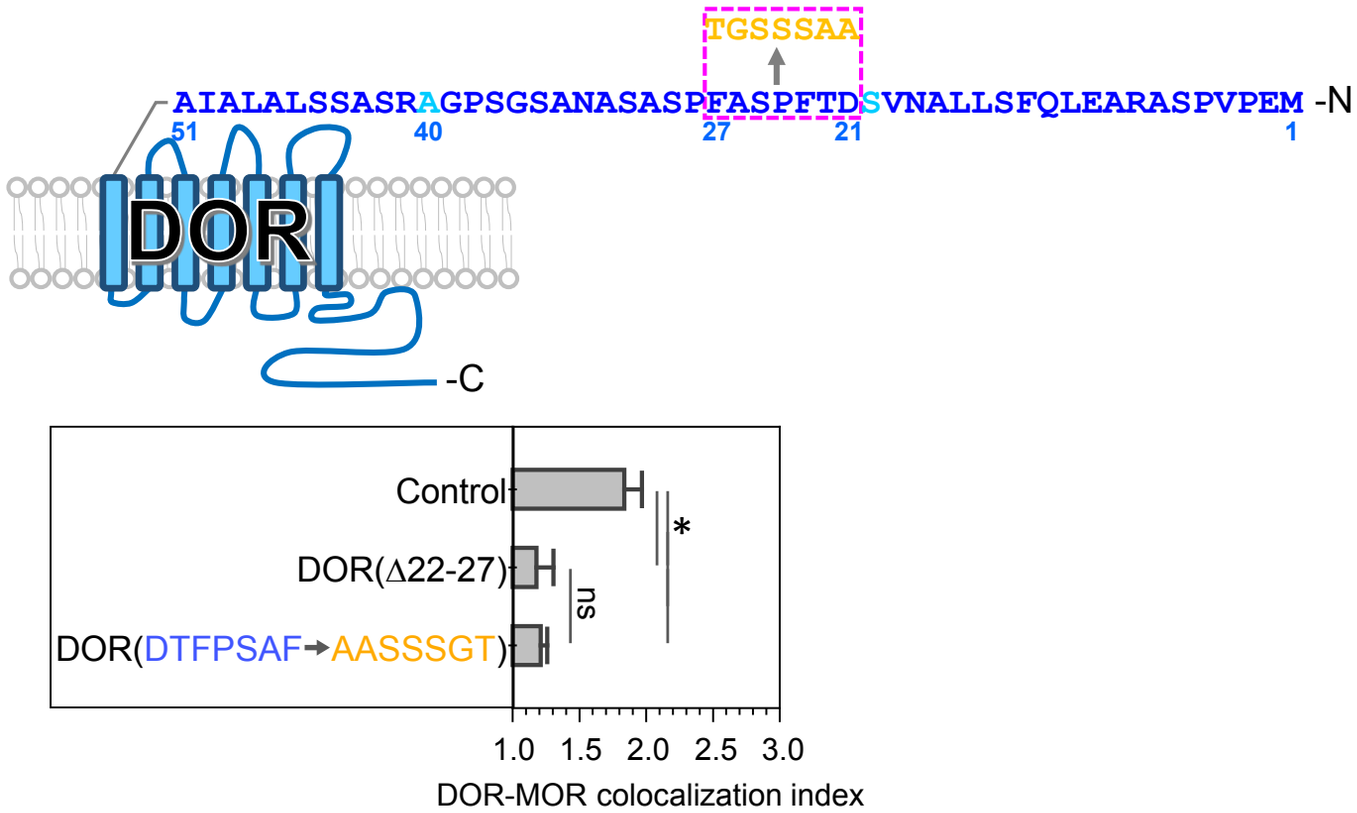
TGSSSAA
AIALALSSASRAGPSGSANASASPFASPFTDSVNALLSFQLEARASPVPEM -N
51
40
27
21
1
DOR
-C
Control
DOR(Δ22-27)
DOR(DTFPSAF→AASSSGT)
*
ns
1.0
1.5
2.0
2.5
3.0
DOR-MOR colocalization index

Figure S4

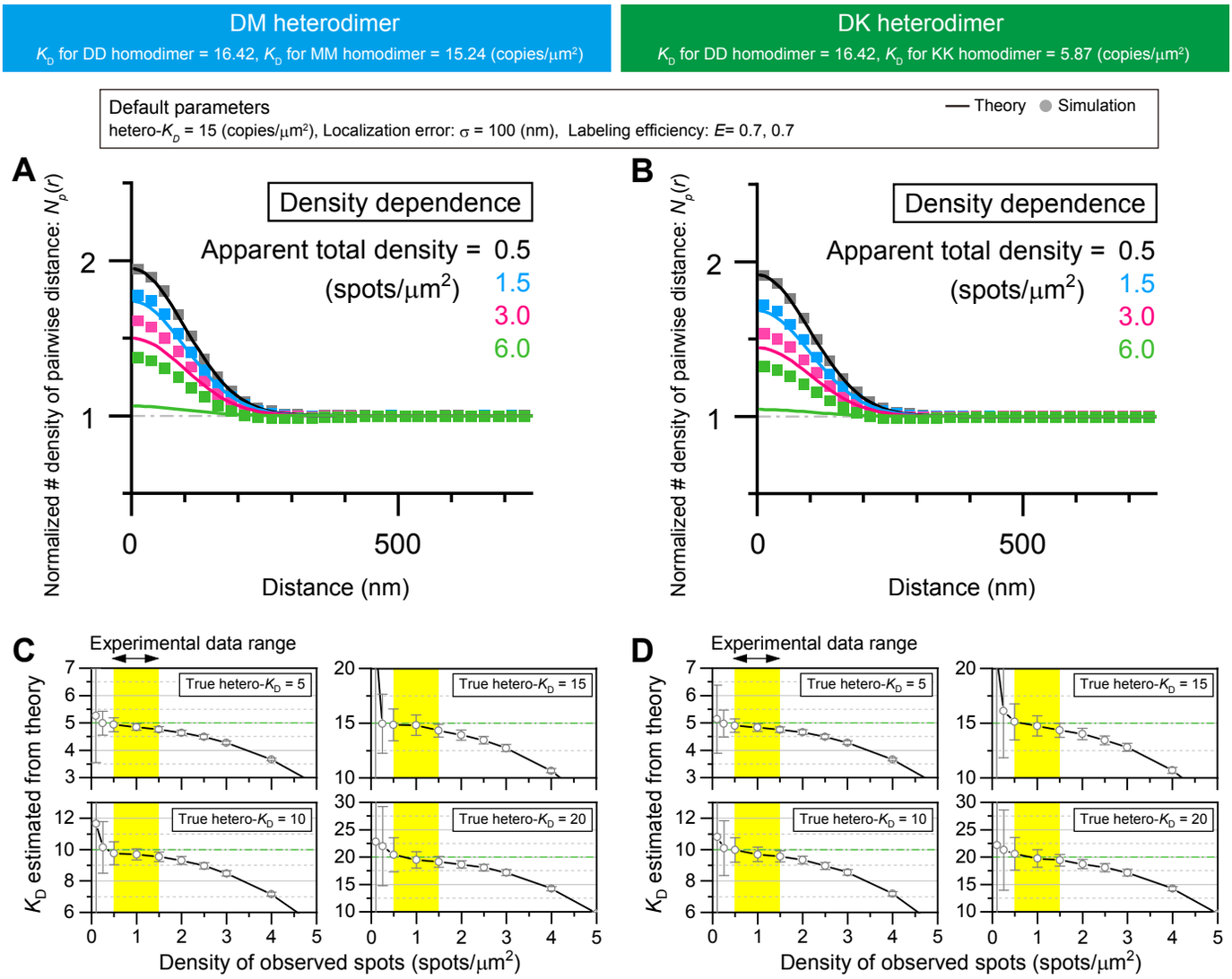
DM heterodimer
K_D for DD homodimer = 16.42, K_D for MM homodimer = 15.24 (copies/μm²)
DK heterodimer
K_D for DD homodimer = 16.42, K_D for KK homodimer = 5.87 (copies/μm²)
Default parameters
hetero-K_D = 15 (copies/μm²), Localization error: σ = 100 (nm), Labeling efficiency: E= 0.7, 0.7
Theory
Simulation
A
B
Density dependence
Apparent total density = 0.5
(spots/μm²) 1.5
3.0
6.0
Normalized # density of pairwise distance: $N_p(r)$
Distance (nm)
C
D
Experimental data range
True hetero-K_D = 5
True hetero-K_D = 15
True hetero-K_D = 10
True hetero-K_D = 20
K_D estimated from theory
Density of observed spots (spots/μm²)

Figure S5

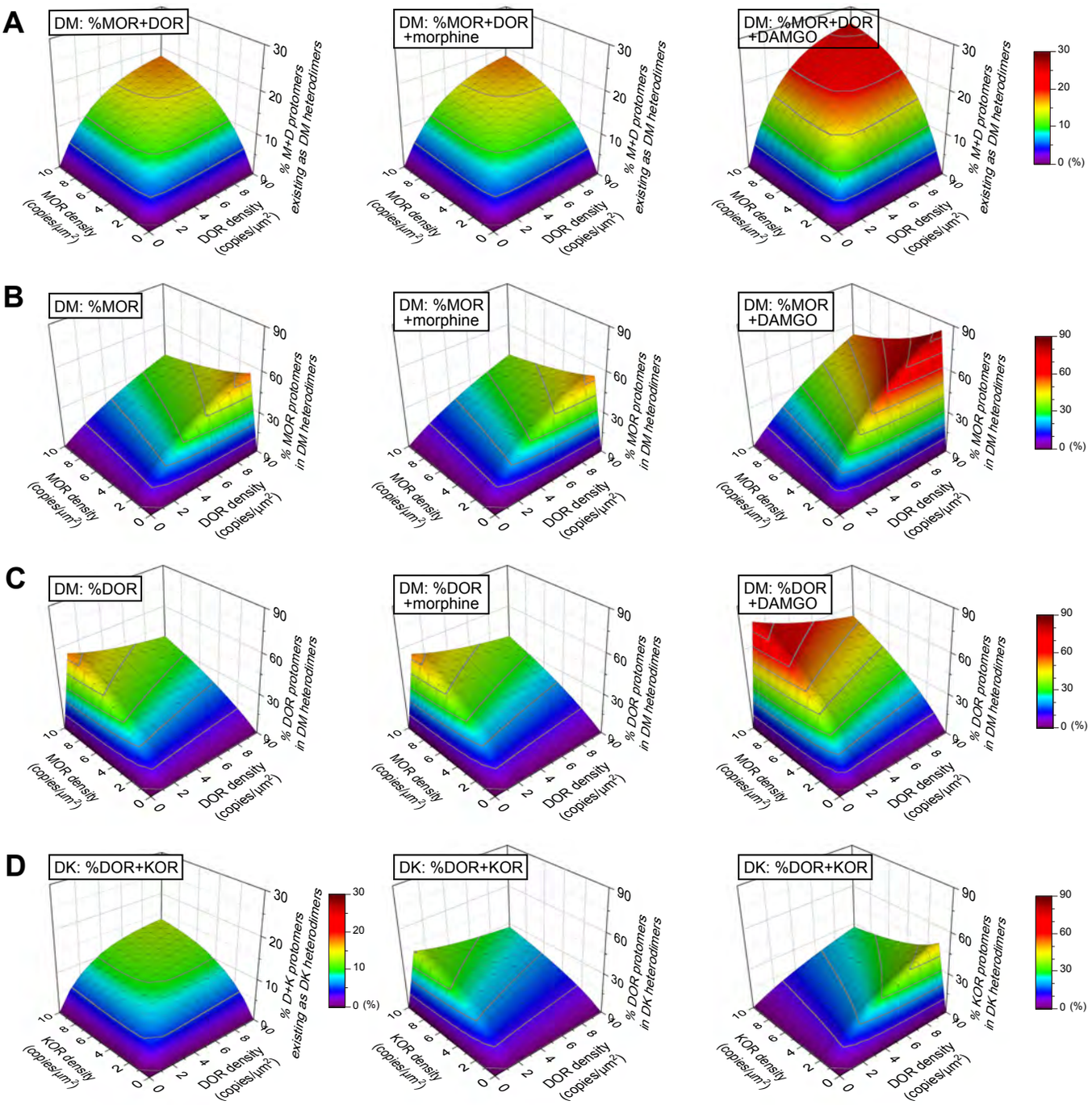
A
DM: %MOR+DOR
DM: %MOR+DOR +morphine
DM: %MOR+DOR +DAMGO
% M+D protomers existing as DM heterodimers
MOR density (copies/μm²)
DOR density (copies/μm²)
0 (%)
B
DM: %MOR
DM: %MOR +morphine
DM: %MOR +DAMGO
% MOR protomers in DM heterodimers
C
DM: %DOR
DM: %DOR +morphine
DM: %DOR +DAMGO
% DOR protomers in DM heterodimers
D
DK: %DOR+KOR
% D+K protomers existing as DK heterodimers
% DOR protomers in DK heterodimers
% KOR protomers in DK heterodimers
KOR density (copies/μm²)

Figure S6

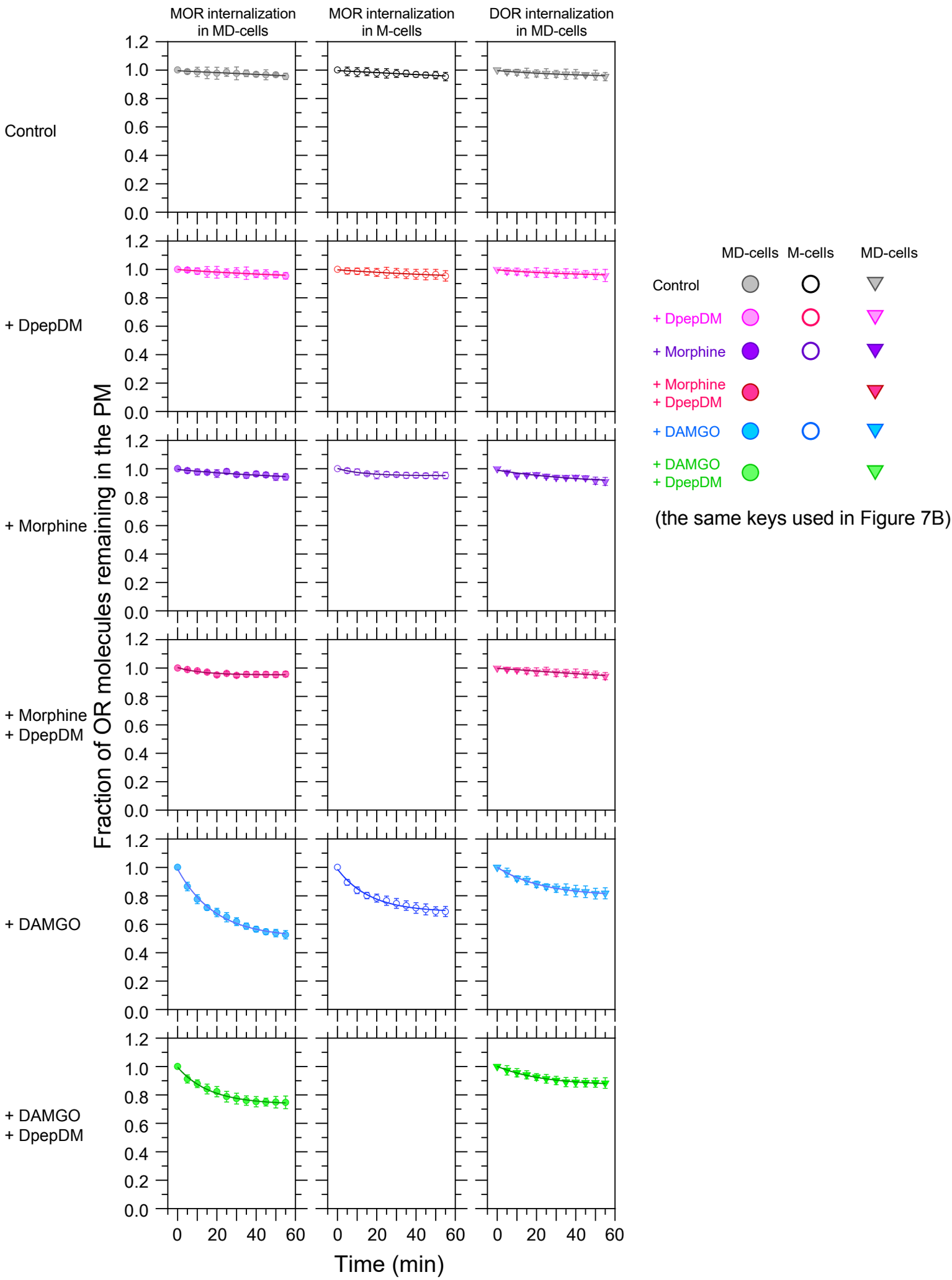
MOR internalization in MD-cells
MOR internalization in M-cells
DOR internalization in MD-cells
Control
+ DpepDM
+ Morphine
+ Morphine + DpepDM
+ DAMGO
+ DAMGO + DpepDM
Fraction of OR molecules remaining in the PM
Time (min)
MD-cells
M-cells
MD-cells
(the same keys used in Figure 7B)

Figure S7

A Dpep(20-42)DM suppresses the DM co-internalization induced by SNC-80

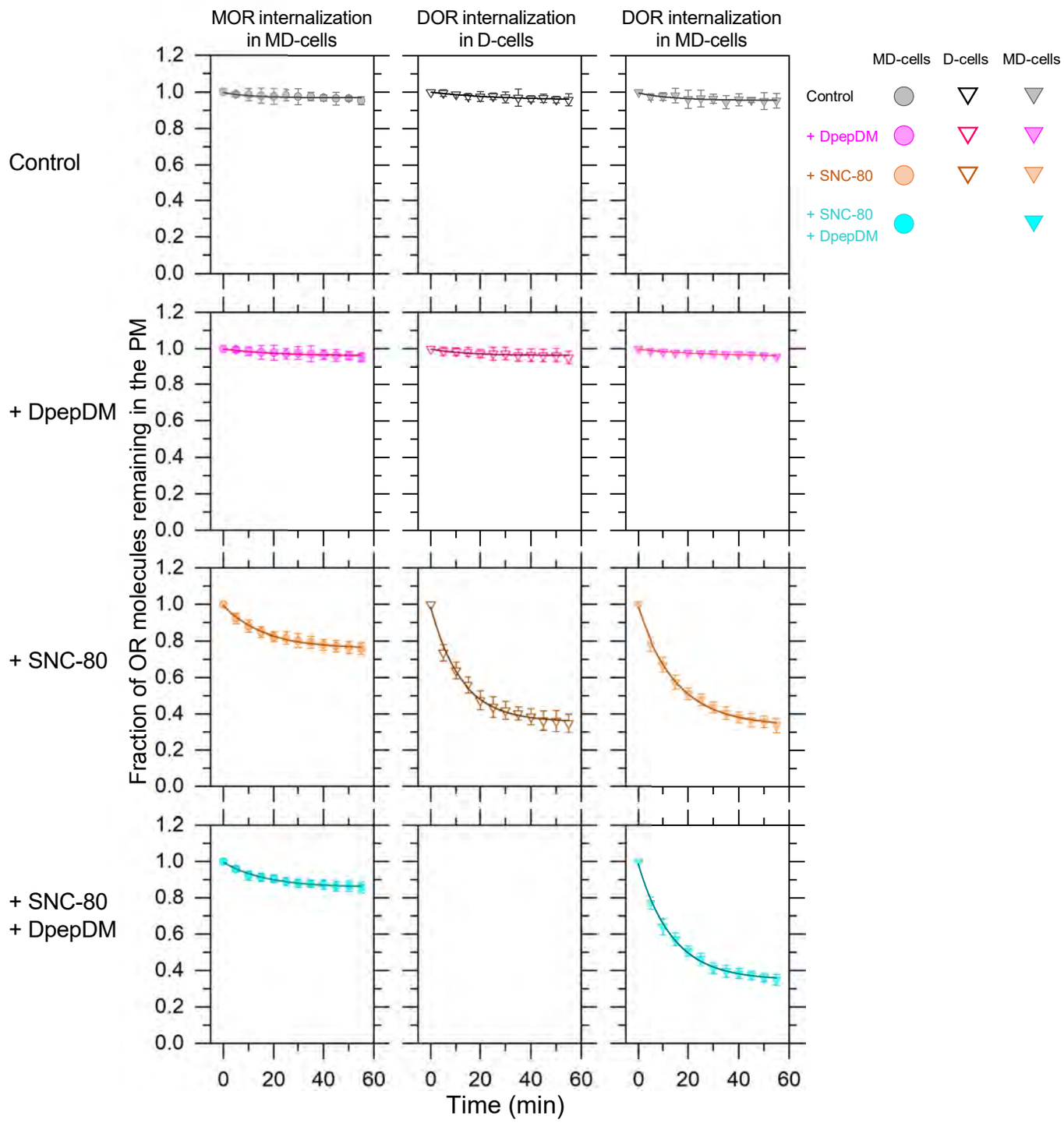

B Dpep(20-42)DM suppresses the development of morphine tolerance

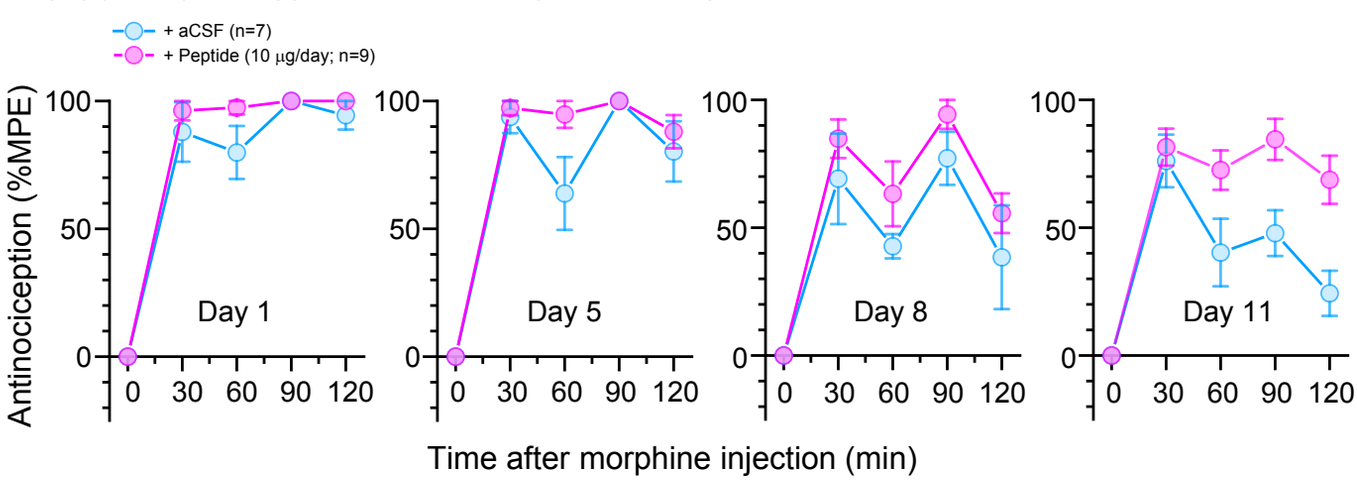

Single-molecule detection of transient dimerization of opioid receptors 2: Heterodimer blockage reduces morphine tolerance

Peng Zhou[1], Rinshi S. Kasai[2,3,4], Wakako Fujita[5,6], Taka A. Tsunoyama[1], Hiroshi Ueda[7,8], Simone Pigolotti[9], Takahiro K. Fujiwara[10], and Akihiro Kusumi[1,10]

[1]Membrane Cooperativity Unit, Okinawa Institute of Science and Technology Graduate University, Onna-son, Okinawa 904-0495, Japan. [2]Institute for Life and Medical Sciences, Kyoto University, Kyoto 606-8507, Japan. [3]Division of Advanced Bioimaging, National Cancer Center Research Institute, Tokyo 104-0045, Japan. [4]Institute for Glyco-core Research (iGCORE), Gifu University, Gifu 501-1193, Japan. [5]Department of Medical Pharmacology, Nagasaki University Graduate School of Biomedical Sciences, Nagasaki 852-8520, Japan. [6]Laboratory of Pharmacotherapeutics, Faculty of Pharmacy, Juntendo University. Urayasu, 279-0013, Japan. [7]Laboratory for the Study of Pain, Research Institute for Production Development, Kyoto 606-0805, Japan. [8]Department of Pharmacology, National Defense Medical Center, Nei-Hu 114, Taipei, Taiwan. [9]Biological Complexity Unit, Okinawa Institute of Science and Technology Graduate University, Onna-son, Okinawa 904-0495, Japan. [10]Institute for Integrated Cell-Material Sciences (WPI-iCeMS), Kyoto University, Kyoto 606-8501, Japan.

Graphical Abstract

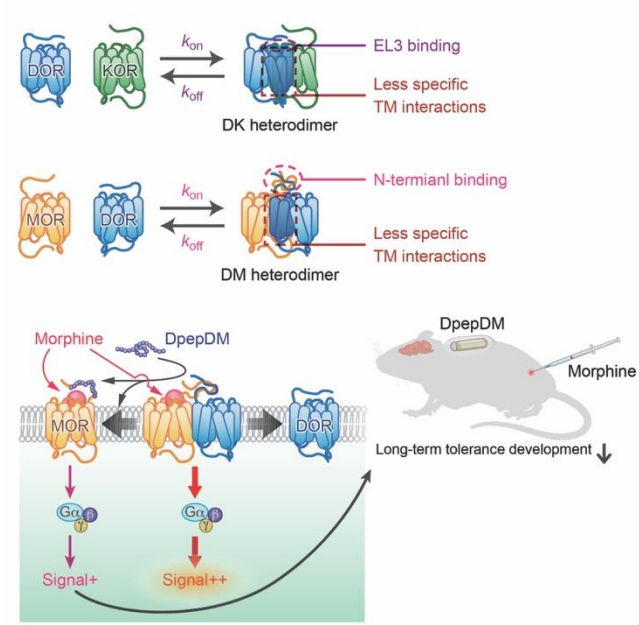

Highlights

- Transient δ-μ and δ-κ, not μ-κ, heterodimers of opioid receptors repeatedly form
- Heterodimerization sites exist in exodomains, and TM sites work less specifically
- Transient heterodimers of agonist-bound μ with δ emit stronger pulse-like signals
- δ-μ blocking peptide reduces tolerance after repeated morphine treatments in mice

Summary

Heterodimerization of opioid receptors (ORs), MOR, KOR, and DOR, is implied in their functional regulation and diversification, and thus its understanding is crucial for developing better analgesic treatments. However, our knowledge on OR heterodimerization/heterodimers remains limited. Here, using single-molecule imaging and functional analysis, we found that MOR, the main morphine receptor, repeatedly forms *transient (≈250 ms) heterodimers* with DOR every 1-10 seconds, but not with KOR, whereas DOR and KOR also form transient heterodimers. We obtained all the heterodimer-monomer equilibrium constants and rate constants with/without agonists. We identified the critical heterodimer binding sites in the extracellular domains, in addition to the less-specific transmembrane domains, and developed soluble peptide blockers for MOR-DOR and DOR-KOR heterodimerization, using amino-acid sequences mimicking the extracellular binding sites. With these peptide blockers, we dissected the monomer/dimer roles in OR internalization and signaling. The soluble MOR-DOR heterodimer blocker reduced the development of long-term morphine tolerance in mice.

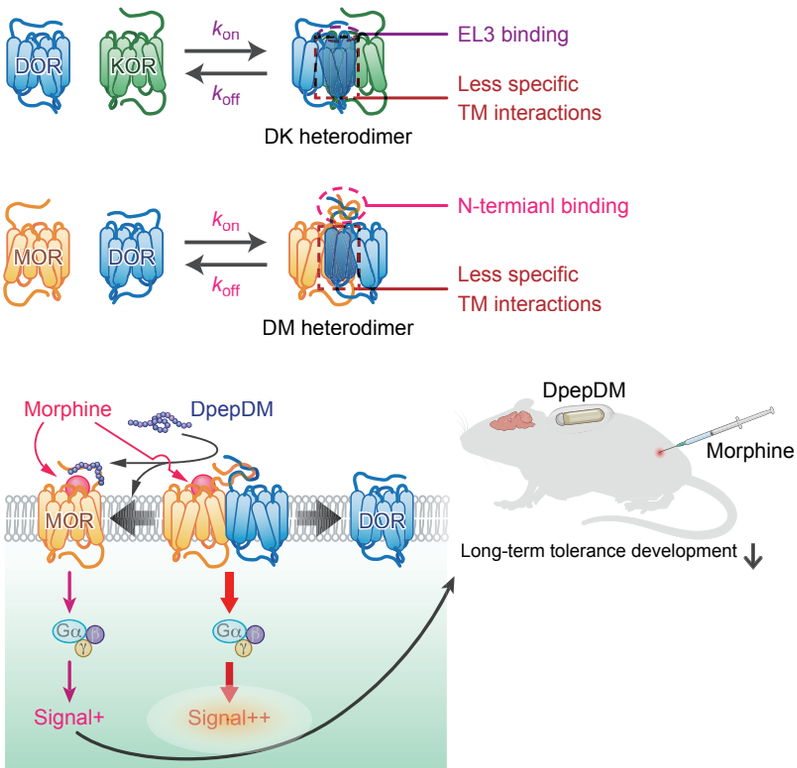
DOR
KOR
k_{on}
k_{off}
EL3 binding
Less specific
TM interactions
DK heterodimer
MOR
DOR
k_{on}
k_{off}
N-termianl binding
Less specific
TM interactions
DM heterodimer
Morphine
DpepDM
MOR
DOR
Gα
β
γ
Signal+
Signal++
DpepDM
Morphine
Long-term tolerance development